NASA TECHNICAL
REPORT

NASA TR R-438

MULTILAYERED MODELS
FOR ELECTROMAGNETIC
REFLECTION AMPLITUDES

William I. Linlor

Ames Research Center

Moffett Field, Calif. 94035

1. Report No. TR R-438	2. Government Accession No.	3. Recipient's Catalog No.
4. Title and Subtitle MULTILAYERED MODELS FOR ELECTROMAGNETIC REFLECTION AMPLITUDES		5. Report Date March 1976
		6. Performing Organization Code
7. Author(s) William I. Linlor		8. Performing Organization Report No. A-5862
		10. Work Unit No. 177-54-11-01
9. Performing Organization Name and Address Ames Research Center Moffett Field, Calif. 94035		11. Contract or Grant No.
		13. Type of Report and Period Covered Technical Report
12. Sponsoring Agency Name and Address National Aeronautics and Space Administration Washington, D. C. 20546		14. Sponsoring Agency Code

15. Supplementary Notes

16. Abstract

    The remote sensing of snowpack characteristics with surface installations or with an airborne system could have important applications in water resource management and flood prediction. To derive some insight into such applications, the electromagnetic response of multilayered snow models is analyzed. Normally incident plane waves are assumed at frequencies ranging from 10^6 to 10^{10} Hz, and amplitude reflection coefficients are calculated for models having various snow-layer combinations, including ice sheets. Layers are defined by a thickness, permittivity, and conductivity; the electrical parameters are constant or prescribed functions of frequency. To illustrate the effect of various layering combinations, results are given in the form of curves of amplitude reflection coefficients versus frequency for a variety of models. Under simplifying assumptions, the snow thickness and effective dielectric constant can be estimated from the reflection coefficient variations as a function of frequency.

17. Key Words (Suggested by Author(s)) Remote sensing, snow, snowpack, water equivalent, water content, wetness, layers, layering, ice, reflection coefficient, multilayers, frequency, electrical parameters, plane waves, dielectric constant, loss tangent, conductivity, water resource management, Fresnel zone, frequency dependence, normal incidence.	18. Distribution Statement Unlimited STAR Category - 43		
19. Security Classif. (of this report) Unclassified	20. Security Classif. (of this page) Unclassified	21. No. of Pages 55	22. Price* $4.25

SYMBOLS

d layer thickness, m

d_e electrical thickness, m

E electrical field amplitude, V/m

E_p electric field vector, V/m

f frequency, Hz

H aircraft altitude, m

j complex notation symbol

K dielectric constant, dimensionless

N normality (equivalents of solute per liter), numeric

n integer, dimensionless

R power reflection coefficient per unit incident, dimensionless ratio

r reflection amplitude per unit incident, dimensionless ratio

S Fresnel zone area, m^2

$\tan \delta$ loss tangent, dimensionless ratio

W volume percent wetness, numeric

Z complex impedance, ohms

Z_a surface impedance, ohms

Z_0 characteristic impedance, ohms

α $2\pi/\lambda$, rad/m

ϵ_0 permittivity of free space (8.854×10^{-12} F/m)

ϵ' permittivity, F/m

ϵ'' loss factor, F/m

ϵ^* complex permittivity, F/m

λ   wavelength, m

μ   permeability, H/m

μ_0 permeability of free space (1.257×10^{-6} H/m)

ρ   density, g/cm^3

σ' conductivity, mho/m

φ   phase angle, rad

ω   angular frequency, rad/sec

MULTILAYERED MODELS FOR ELECTROMAGNETIC REFLECTION AMPLITUDES

William I. Linlor

Ames Research Center

SUMMARY

The remote sensing of snowpack characteristics with surface installations or with an airborne system could have important applications in water resource management and flood prediction. To derive some insight into such applications, the electromagnetic response of multilayered snow models is analyzed. Normally incident plane waves are assumed at frequencies ranging from 10^6 to 10^{10} Hz, and amplitude reflection coefficients are calculated for models having various snow-layer combinations, including ice sheets. Layers are defined by a thickness, permittivity, and conductivity; the electrical parameters are constant or prescribed functions of frequency. To illustrate the effect of various layering combinations, results are given in the form of curves of amplitude reflection coefficients versus frequency for a variety of models. Under simplifying assumptions, the snow thickness and effective dielectric constant can be estimated from the reflection coefficient variations as a function of frequency.

INTRODUCTION

With water supplies and the hydroelectric power obtained from them in great demand, the water equivalent of snowpacks represents an important resource on a worldwide basis. The effective management of water resources requires adequate knowledge of the snowpack extent, depth, density, and wetness. At present, trained individuals traverse snow courses to obtain snow depth and weight using Mt. Rose tubes at selected sites. Some additional information is obtained by the use of "pressure pillows" to weigh the snow at automatic stations; other systems involve the attenuation of gamma rays by absorption in snow layers.

The field methods in current use are of great value in providing information to permit forecasting of water runoff; "point" measurements are combined by statistical methods to yield a representative value for a basin. However, automatic stations and airborne systems for repetitive assessment of snowpack depth, density, and wetness would have important applications in water resource management and flood prediction, particularly at times of rapid change. Other applications involving airborne or satellite-based techniques include measurement of ice thickness on shipping lanes and in the polar regions, and snow cover on remote areas.

Remote sensing systems are being developed by the scientific community, based on both passive and active electromagnetic (EM) techniques. Considerable literature is already available; particularly relevant to this paper are references 1–5. A "swept-frequency" EM system for snowpack measurements is described by Linlor (ref. 6), for which the models analyzed in the present paper represent the theoretical basis. In a simple form, that system would consist of an antenna that transmits a set of sequential fixed frequencies (thus approximating a "swept-frequency" operation).

A selected frequency would be transmitted within a pulse having sufficient duration to include between 10 and 100 cycles, thus nearly equivalent to "continuous wave" (CW) operation. With the antenna on an aircraft at an altitude of 150 m or higher, the pulse having a duration of 1 μsec or less would be completed before the specular reflection from the snowpack could reach the antenna. Hence, the same antenna could be used for transmission and reception. Amplitude and phase of the reflected signals would be recorded for the desired frequency range.

The present work is part of a broad program having many interdependent aspects. The ultimate goal is a remote-sensing system that can be flown in an aircraft or satellite to obtain repetitive, synoptic measurements of snowpack areal extent, depth, density, and wetness. Combinations of passive and active EM instrumentation are envisaged, the latter including short-pulse as well as the pulsed swept-frequency measurements described above. For flight experiments, ground truth is needed, and suitable instrumentation to obtain such information is being developed. Snow wetness, which is one of the most important parameters determining the EM response, may be measured at the surface by electrical techniques described in references 7 and 8.

Our proposed active EM airborne remote-sensing system is a direct spinoff from some of the basic research in the NASA space exploration program. Prior to the Apollo 17 mission, theoretical analyses and computer codes were used to obtain the response of (hypothetical) plane layers on the moon, assuming incident plane EM waves, as described in references 9 and 10.

During the manned lunar exploration program, consideration was given to application of the EM techniques to various layered models of snow, ice, water, and earth, and certain problems inherent in such applications were recognized. The electrical parameters of snow, *in situ*, are known to cover a wide range of values depending on the density, temperature, free-water content, and other variables such as sequences of rain, freezing, and thawing. There also are important practical considerations, such as the effects of earth roughness, snow surface roughness, reflection from inadvertent radiators (telephone or power lines in the vicinity of the reflection zone), and similar complications. A few remarks are made later in this paper concerning the limitations arising from practical applications.

As an initial step, this paper is a theoretical study only, and does not include consideration of the size, weight, cost, or performance characteristics of a working system. The basic objective is to present the results of calculations for a variety of models, directed toward such questions as:

1. For sets of earth conditions, how does the reflection coefficient depend on the dielectric constant, loss tangent, and thickness of the snow layers?

2. For various sets of snow layers, how does the reflection coefficient depend on the dielectric constant and loss tangent of the earth?

3. For an invariant amount of water-equivalent in the totality of the layers, how does the reflection coefficient change when the individual layers of snow (or ice) are interchanged in various sequences?

The author is indebted to Dr. George Jiracek of the University of New Mexico for help in adapting the computer code to the present set of models.

OUTLINE OF THEORY

The principle of the electromagnetic interactions on which the proposed system is based can be explained by the model shown in figure 1. The model represents the simple case of a thin sheet separating two semi-infinite media. Stratton (ref. 11) derives the following expression for the reflection coefficient at normal incidence assuming that the three media have zero conductivity and vacuum permeability:

$$R = \frac{(r_{12} + r_{23})^2 - 4r_{12}r_{23} \sin^2 \alpha_2 d}{(1 + r_{12}r_{23})^2 - 4r_{12} r_{23} \sin^2 \alpha_2 d} \tag{1}$$

where the amplitude reflection coefficients at the interfaces are r_{12} and r_{23}, d is the sheet thickness, and $\alpha_2 = 2\pi/\lambda_2$ where λ_2 is the wavelength within the sheet. The power reflection coefficient R is what an airborne instrument would measure and is given by

$$R = r^2 \tag{2}$$

where r represents the amplitude reflection coefficient for the model. Unless explicitly stated otherwise, we use amplitude reflection coefficients in this paper.

The sequential minima for r occur at the frequencies

$$f = \frac{3 \times 10^8}{4d\sqrt{K_2}} (2n + 1) \qquad n = 0, 1, 2, 3, \ldots \tag{3}$$

$$r_{min} = \frac{\sqrt{K_1 K_3} - K_2}{\sqrt{K_1 K_3} + K_2} \tag{4}$$

$$K_i = \frac{\epsilon_i}{\epsilon_O} \qquad i = 1, 2, 3 \tag{5}$$

where f is the frequency in Hz and d is the thickness in meters. The permittivities of the three dielectrics are ϵ_1, ϵ_2, and ϵ_3 in F/m, and the dielectric constants are K_1, K_2, and K_3, which are dimensionless.

For the assumed lossless media, the maxima for r are equal to r_{13}, namely, the reflection coefficient with layer 2 effectively absent; these occur at the sequential frequencies

$$f = \frac{3 \times 10^8}{4d\sqrt{K_2}} (2n + 2) \qquad n = 0, 1, 2, 3, \ldots \tag{6}$$

$$r_{max} = r_{13} = \frac{\sqrt{K_3} - \sqrt{K_1}}{\sqrt{K_3} + \sqrt{K_1}} \tag{7}$$

3

Letting $K_1 = 1.0$ for air, from equations (4) and (7) we obtain

$$K_2 = \frac{1 + r_{max}}{1 - r_{max}} \times \frac{1 - r_{min}}{1 + r_{min}} \qquad (8)$$

$$K_3 = \left(\frac{1 + r_{max}}{1 - r_{max}}\right)^2 \qquad (9)$$

A solid ice layer over water is an example of a three-layer system. Let us make the simplifying assumptions that the ice and water are lossless, and have dielectric constants of 3.2 and 81, respectively, independent of frequency. A plot of equation (1) is shown in figure 2, with thickness d of medium 2 plotted in units of λ_2, versus amplitude reflection coefficient of the model. For ice thickness equal to a quarter wavelength, the amplitude reflection coefficient for this model is equal to 0.47. If medium 2 had a dielectric constant of $\sqrt{K_3}$ (i.e., 9), the reflection amplitude of the system would be zero for odd multiples of the quarter wavelength thickness.

Figure 3 is a plot of equation (1) for the amplitude reflection coefficient r versus frequency for an ice layer assumed to be 0.03 m thick. The first minimum in r occurs at the frequency of $f_1 = 1.40 \times 10^9$ Hz; adjacent minima have a frequency difference of

$$\Delta f = \frac{3 \times 10^8}{2d \sqrt{K_2}} = 2f_1 \qquad (10)$$

It is obvious for this idealized example that the variation of the amplitude reflection coefficient with frequency shown in figure 3 is sufficient to determine uniquely the dielectric constants of the ice and water from equations (8) and (9), and the thickness of the ice layer from equation (3) or (10).

It should be noted that figure 3 represents steady-state (CW) frequencies; that is, pulsing the incident wave is not necessary except for operational convenience. The effects that occur are "interferometric" in nature, and minima can be explained by considering a frequency such that the wavelength in the ice is four times the thickness of the ice. For this condition, the EM wave, in traversing the ice layer down and up, accumulates a time delay so that the phase of the wave emerging from the top surface of the ice is 180° with respect to the surface reflected wave. Because of the significant amount of reflection at the ice-water boundary, the amount of cancellation at the top surface is sufficiently great so that the net amplitude reflection coefficient is 0.47 at the frequency of 1.40×10^9 Hz. This same type of phase relationship occurs at the odd multiples (1, 3, 5, 7, etc.) of this frequency, producing minima in the amplitude reflection coefficients at the frequencies (GHz) of 1.40, 4.20, 7.00 . . .

At the even multiples (2, 4, 6, etc.) of the frequency 1.40×10^9 Hz, the internally reflected wave emerging from the ice top surface is in phase with the surface reflected wave, so constructive interference occurs. In other words, at these even multiples the amplitude reflection coefficient is the same as if the ice were absent — that is, equal to 0.80, which is obtainable directly from equation (7) using the value of 81 for the dielectric constant of water and of unity for air.

Let us now consider multilayered models. The mathematical analysis has been published by Ward et al. (ref. 9) and is not repeated here. The same computer code was used for the calculations

4

of this paper, modified to include as many as 48 separate layers, each of which can have permittivity and conductivity values that vary with frequency. Relations presented in reference 9 are used in this discussion as appropriate.

It is assumed that plane electromagnetic waves are incident normally on plane layers, each of which is homogeneous within its upper and lower surfaces. The permittivity ϵ' and conductivity σ' of each layer are real functions of frequency f; the magnetic permeability μ of all materials is the same as that for vacuum. The layers extend indefinitely in the horizontal plane, and the incident waves have sinusoidal time variations.

With the usual nomenclature, the complex permittivity is

$$\epsilon^* = \epsilon' + j\epsilon'' \tag{11}$$

The electrical conductivity is related to the loss factor ϵ'' by

$$\sigma' = 2\pi f \epsilon'' \tag{12}$$

The ratio of conduction current to displacement current in each layer is the loss tangent:

$$\tan \delta = \frac{\sigma'}{\omega \epsilon'} = \frac{\epsilon''}{\epsilon'} \tag{13}$$

For a given model, the surface impedance is defined to be Z_a, which is equal at any selected frequency to the impedance of an equivalent homogeneous half-space. The plane wave impedance of free space is Z_O. The amplitude reflection coefficient for the multilayered model is

$$r = \frac{Z_a - Z_O}{Z_a + Z_O} \tag{14}$$

The phase angle ϕ_a and modulus $|Z_a|$ of the complex impedance Z_a are related by

$$Z_a = |Z_a| e^{j\phi_a} \tag{15}$$

Apparent values for conductivity and permittivity are defined for the model by

$$\sigma'_a = \frac{\mu_O \omega}{|Z_a|^2} \sin 2\phi_a \tag{16}$$

$$\epsilon'_a = \frac{\mu_O}{|Z_a|^2} \cos 2\phi_a \tag{17}$$

The phase angle ϕ_a is zero for an EM wave incident on a loss-free dielectric half-space, and is 45° for an EM wave incident on a conductor in which dielectric displacement currents are negligible. For a lossy, layered model, the phase may range from negative through positive angles as the frequency is varied.

5

In the remainder of this paper, only the amplitude reflection coefficient r is examined as a function of frequency for illustrative models. The computer calculations cover the frequency range of 10^6 to 10^{10} Hz. Values of conductivity and dielectric constant are specified at the beginning of each decade, and interpolation is made by the computer as a power function within each decade.

Results are given in the form of curves of amplitude reflection coefficients r vs frequency f for selected models. A variety of earth types and snow-layer combinations has been chosen to illustrate the effect on the r vs f curve, and we have purposely prescribed a considerable range in snow and earth electrical parameters. The specifications of permittivity and conductivity for snow and earth types do not necessarily describe real specimens.

It should be noted that the "forward" solution, which calculates r vs f curves for a prescribed model, gives unique results. However, considering the "inverse" problem, if a certain r vs f curve is specified (or obtained by field measurements of the reflection vs frequency), the calculation of a model is, in general, not unique. Various mathematical techniques used for the inverse problem have been published; for example, see reference 12.

The basic objective of this paper is to present r vs f curves for a variety of models to show the sensitivity of EM reflection under different conditions. This heuristic approach can be useful in many ways. For example, it can serve as a guide, if other considerations are favorable, to selection of frequency ranges in a contemplated experiment. This is particularly important to avoid "data aliasing" produced by insufficient sampling, that is, by measurements too coarse in frequency. Conversely, unnecessarily fine steps in frequency can be identified and avoided for economical reasons. More generally, the r vs f curves are relevant to all radio-echo sounding amplitudes, inasmuch as even short pulses can be Fourier analyzed into steady-state frequency distributions. Passive microwave measurements may be affected by the layering of the target region, in which case inclusion of interference effects to be presented in the following material may be necessary for proper interpretation of the results.

ELECTRICAL PARAMETERS

A relation for the dielectric constant K, density ρ in g/cm^3, and liquid-phase water (or wetness W) of snow (in volume percent) is given by Ambach and Denoth (ref. 13) as follows:

$$K = 1.00 + 2.22\rho + 0.213W \tag{18}$$

A slightly modified form of the preceding equation, which is based on our field tests of snow electrical properties, is used in this paper:

$$K = 1.00 + 2.00\rho + 0.213W \tag{19}$$

and is assumed to be independent of frequency in the range of 10^6 to 10^{10} Hz. In this frequency range, solid ice is assumed to have a dielectric constant of 3.2, independent of frequency.

To display the effects of various conductivities and dielectric constants, we have arbitrarily postulated the seven types of snow listed in table 1; values for ice are also included. These are

intended to include the range of snow parameters likely to be encountered in field situations. For dry snow (A, B, and C, table 1), we use the relation between loss tangent and frequency given by Figure VII-8 of Mellor (ref. 14); for moisture-free ice, we use figure 7 of Evans (ref. 15); the values are given in table 1.

The data given in figure 5 of Cumming (ref. 2) are used for the effect of liquid-phase water in snow (D, E, F, and G, table 1). Our computer calculations require only the values at the end frequencies 10^9 and 10^{10} Hz. For values within this range, linear interpolation on the logarithmic scale (i.e., a power function) is done by the computer. Thus, for snow having volume percent wetness equal to or greater than 1 percent, we use the following relations:

$$\tan \delta = 5.00 \times 10^{-3} W \text{ at } 10^9 \text{ Hz} \tag{20}$$

$$\tan \delta = 3.16 \times 10^{-2} W \text{ at } 10^{10} \text{ Hz} \tag{21}$$

The earth electrical values in table 1 are quite arbitrary. Earths I, I*, II, and III are assumed to have tan δ values that are constant in the frequency range of 10^6 to 10^{10} Hz. Earths IV, V, VI, and VII are approximations to "real" earths, VI being more conductive. The ranges of electrical values, although arbitrary, are intended to include most of the commonly occurring earths.

The electrical parameters are shown in figure 4 for snow and ice and in figure 5 for earth and water.

It should be noted that the selected electrical parameters of snow, ice, and earth do not necessarily represent actual physical specimens. Rather the various types are assumed media, selected to encompass the range of electrical parameters that can be expected in reality. In a flight experiment, one would periodically take data over suitable sites prior to and immediately after the first significant snowfall to determine the conductivity and dielectric constant of the earth as functions of frequency.

MODELS

We start with the "half-space" response of the various types of earth, snow, ice, and water. To avoid repetition of the phrase "reflection amplitude" we employ the notation r. As mentioned earlier, one obtains the power reflection coefficient, per unit incident intensity, by squaring r.

After consideration of the half-space response we proceed to successively more complicated configurations, namely three-, four-, and multi-layered models. In all of the calculations of this paper, no approximations are made based on tan δ being much smaller or much greater than unity; indeed, values for tan δ close to unity are of interest for many of the calculations.

The description of the models is facilitated by defining a format for the layers. The various snows are identified by the letters A through G, and the various earth types are identified by Roman numerals I through VII; the thickness of any snow or ice layer is identified by the value given in parentheses; the sequence is identified by the use of diagonals, starting with the top layer. For example, a layer of snow B, 1.0 m thick, on top of a layer of snow D, 0.2 m thick, on top of a

layer of ice 0.2 m thick, on top of earth type IV would be designated:

B(1.0)/D(0.2)/Ice (0.2)/IV

HALF-SPACE RESPONSES

The values of r versus frequency for earths I through VII are shown in figure 6. The r-values for earths I, II, and III are independent of frequency because of the assumption that the dielectric constant and tan δ values are independent of frequency. With the exception of earth VI, the values of r are essentially determined by the dielectric constant for frequencies above about 10^7 Hz. Earth VI, which represents a water-saturated and therefore highly conducting earth, exhibits r-values that are frequency-dependent over the entire range of interest.

Also shown on figure 6 is the half-space response of water, assumed to be 0° C and having conductivity corresponding to 0.001 N NaCl. The values of r are essentially constant above 10^8 Hz.

For snows A through G and for ice, the r values are so nearly independent of frequency that we present the results in table 2, rather than in a graph. The conclusion from the half-space responses is that the r-values are *monotonic functions of frequency*.

THREE-LAYER MODELS: SNOW ON EARTH

The r-values for 1 m of snows A through G on earths IV and VI are given in tables 3 and 4, respectively, for the frequency range 10^6 to 10^7 Hz, together with the r-values in the absence of snow. Similar information for 2 m of snows B, C, and G on earths II and III is given in table 5.

The information supports the conclusion that for wavelengths much longer than the snow thickness, the r-value is determined by the half-space response of the earth.

The r-values for 1 m of snows A through G on earths IV, V, and VI are shown in figures 7–13 for 10^7 to 10^8 Hz. Each figure displays a given type of snow, 1 m thick, on top of these three earth types. For earth types IV and V, each with a dielectric constant of 10, the r-values are not significantly affected by the earth tan δ values.

The information is consistent with the equation for the frequency at which the first minimum occurs:

$$f_1 = \frac{3 \times 10^8}{4d\sqrt{K}} \text{Hz} \tag{22}$$

Equation (22) is based on the assumption that the snow layer and earth do not have conduction currents, so it is only approximate for snow G.

To demonstrate the effect of conduction currents on the earth, figure 14 shows r-values for 1 m of snow C over earth I and over earth III. Both of these earth types have dielectric constants of 10;

8

earth I, with loss tangent of 10^{-2}, can be considered to be loss-free, but earth III has loss tangent of unity, and therefore its conduction current equal its displacement current.

Let us now examine the r-values for 1 m of snows A through G over earth IV and over earth VI in the frequency range 1.0×10^9 to 1.4×10^9 Hz. The frequency scale is selected so as to display the curves adequately. We recall that for lossless media, the difference in frequency at successive minima is equal to twice the frequency value at which the first minimum occurs. Inspection of figures 15−21 shows this relation to be applicable with a quite high degree of accuracy, even to lossy snow types over lossy earth types. Also we note that for nonlossy snow types, the r-values at the successive maxima are essentially equal to the half-space responses.

The effect of snow lossiness on the r-values is evident in the cases of snows F and G in figures 20 and 21, respectively. Let us explore this effect with further examples, because it furnishes us with a convenient means for measuring the snow wetness. Let us consider the case of 1 m of snow D over earth IV. The r-values are plotted in figures 22−25 for the frequency ranges, each multiplied by 10^9 Hz, of 1.0 to 1.4; 6.0 to 6.4; 7.0 to 7.4; and 8.0 to 10.0. We note that snow D is assumed to have only 1 percent volume wetness, but for the 1-m depth the losses are sufficient to produce essentially a half-space response at frequencies above 8.0×10^9 Hz. Evidently the behavior of the r-values in the 10^9 to 10^{10} Hz range is very dependent on the wetness. As one would expect, for situations in which the snow layer produces increasingly significant attenuation of the waves, the characteristics of the earth layer become progressively less effective in the net response.

For the case of 1 m of snow G over earth VI, the r-values for the frequency range of 2.0 to 10.0×10^9 Hz are essentially the same as for the half-space response, as is displayed in figure 26.

The effect of attenuation in wet snow is further shown in figures 27 and 28, which give plots of the r-values in the frequency range of 10^9 to 10^{10} Hz for snow G with layer thicknesses of 3 cm and 1 cm, respectively. Despite the highly damped waves of figure 27, the spacing of successive minima in frequency is nevertheless essentially equal to twice the frequency at which the first minimum occurs.

For 1 m of snow G over earth VI, the effect of attenuation is evident, but not prohibitively large, in the frequency range 1.0 to 2.0×10^8 Hz, as shown in figure 29.

The attenuation produced by snow types A through G is given in terms of skin depth (i.e., thickness at which the *amplitude* of the wave is reduced by the factor e relative to the amplitude at zero thickness) as a function of frequency in table 6.

Let us now consider briefly snow depths of 2 m. Values of r for snow types A and B over earth types IV and VI are shown in figures 30 and 31. The curves show that the frequencies for the first minima are essentially half as great as the corresponding frequencies in the 1-m depth examples.

This concludes the discussion of single layers of snow over earth. Although the models are relatively simple, we have seen that in some situations the presence of conduction currents in the media affects the electromagnetic response. Such effects are not necessarily undesirable − in fact quite the opposite. The sensitivity of the response to wetness can be a most useful indicator of the snow ripeness and of the earth conditions.

THREE-LAYER MODELS: ICE ON WATER

In this section we consider a few models of ice on water, with the electrical parameters as given in table 1, the impurities in the water being approximately equivalent to 0.001 N aqueous NaCl at 0° C. Previously, a discussion was given in the theoretical section for the case of nonconducting ice and water. The effect of the conductivity is shown in figure 32 for the case of 3 cm of ice over water.

To demonstrate the effect of ice thickness, two curves are shown in figure 33 for the model of 0.10-m ice over water and the model of 0.11-m ice over water. The frequencies at which the first minima occur are related inversely as the ice thickness, a result that is also obtainable from equation (1) or equation (3). For the model of 1.0-m-thick ice over water, the frequency for the first minimum is a factor of 10 smaller than for the model of 0.1-m-thick ice over water. The r-values versus frequency are given in figure 34.

These models indicate that for plane ice layers on water, the swept-frequency r-values provide excellent measures of ice thickness, to the extent that the stated assumptions apply.

MULTILAYERED MODELS

In this section we examine multilayered models such as snow and ice on earth, and hypothetical layers whose dielectric constant is a function of depth. To permit comparison of results the model characteristics are selected so as to preserve certain quantities of interest, for example the "electrical thickness." This is defined to be:

$$\sum_i d_i \sqrt{K_i} = d_e \tag{23}$$

Another quantity of interest is the water equivalent of the model; this is based on the thickness and electrical parameters of any layer being unchanged when the layers are interchanged in some specified way. Of course this automatically preserves the electrical thickness. From here on, the models will be numbered consecutively. Models that are related are grouped together.

Model 1. D(1.0) /Ice (0.2)/I
Model 2. Ice (0.2)/D(1.0)/I

The layer format is interpreted to mean: a layer of snow D, 1 m thick, plus a layer of ice 0.2 m thick, over earth I. In the first model, the snow is on top; in the second model the ice is on top. The r-values for these two models are plotted in figure 35, for the frequency range of 10^7 to 10^8, showing the first dip in the response. The mean of the frequencies at which the first minimum occurs is 4.08×10^7 Hz, the individual frequencies being 4.35×10^7 Hz for model 1 and 3.80×10^7 Hz for model 2. The r-values at the minima are equal for the two models, but the r-values at the maxima are quite different. This is the result of the different impedance gradations between air and earth I for the two models.

Model 3. C(1.0)/Ice (0.2)/I
Model 4. C(0.8)/Ice (0.2)/C(0.2)/I
Model 5. C(0.6)/Ice (0.2)/C(0.4)/I
Model 6. C(0.4)/Ice (0.2)/C(0.6)/I
Model 7. C(0.2)/Ice (0.2)/C(0.8)/I
Model 8. Ice (0.2)/C(1.0)/I
Model 9. Composite (1.2)/I

Models 3 through 8 refer to a layer of ice 0.2 m thick and snow C 1.0 m thick over earth I. The layer of ice is at the bottom (next to the earth) for model 3. For each of the remaining models, the total amount of snow C is constant, but the ice layer is specified to be at successively higher levels, in 0.2-m increments, ending with the ice at the top for model 8. Model 9 refers to a "composite" material, obtained from equation (23), whose thickness is 1.2 m and whose dielectric constant is 2.18; the loss tangent is taken to be similar to that of snow C. Model 9 thus represents a uniform material whose electrical thickness and physical thickness are the same as for models 3 through 8. Earth I is essentially a dielectric (tan δ = 0.01).

Model 10. C(1.0)/Ice (0.2)/III
Model 11. C(0.8)/Ice (0.2)/C(0.2)/III
Model 12. C(0.6)/Ice (0.2)/C(0.4)/III
Model 13. C(0.4)/Ice (0.2)/C(0.6)/III
Model 14. C(0.2)/Ice (0.2)/C(0.8)/III
Model 15. Ice (0.2)/C(1.0)/III
Model 16. Composite (1.2)/III

Models 10 through 15 are similar to models 3 through 8, except that earth III is employed in place of earth I. The tan δ value for III is 1.0, independent of frequency.

The r-values for models 3 through 8 for the frequency range of 10^7 to 10^8 Hz are plotted in figure 36. Although the curves overlap, the effect of the positioning of the ice layer is clear. The r-values for models 10 through 15 are similarly plotted in figure 37. In figure 38, the r-values for models 9 and 16 are plotted, so that the effect of the two different earth types can be compared; also the response of the composite material can be seen. Having the same electrical thickness as the other models, the composite material represents an average impedance for the group of models.

Model 17. D(1.0)/G(1.0)/Ice (0.2)/I
Model 18. D(1.0)/Ice (0.2)/G(1.0)/I
Model 19. Ice (0.2)/D(1.0)/G(1.0)/I

In figure 39 are plotted the r-values in the frequency range of 10^7 to 10^8 Hz for models 17 through 19, which represent a layer of ice, 0.2 m thick, in various positions with regard to a layer of snow D and snow G, each 1.0 m thick, over earth I. The frequency at which the first minimum occurs is essentially the same for all three models.

Model 20. A(0.2)/E(0.2)/B(0.2)/D(0.2)/C(0.2)/Ice (0.2)/III
Model 21. A(0.2)/E(0.2)/B(0.2)/D(0.2)/Ice (0.2)/C(0.2)/III
Model 22. A(0.2)/E(0.2)/B(0.2)/Ice (0.2)/D(0.2)/C(0.2)/III
Model 23. A(0.2)/E(0.2)/Ice (0.2)/B(0.2)/D(0.2)/C(0.2)/III

Model 24. A(0.2)/Ice (0.2)/E(0.2)/B(0.2)/D(0.2)/C(0.2)/III
Model 25. Ice (0.2)/A(0.2)/E(0.2)/B(0.2)/D(0.2)/C(0.2)/III
Model 26. A(0.2)/E(0.2)/B(0.2)/D(0.2)/C(0.2)/III (No ice present)

Models 20 through 25 involve various types of snow, each 0.2 m thick, and an ice layer 0.2 m thick. The ice layer is positioned successively higher in the sequence; this alters the impedance match from air to earth, but preserves both the electrical thickness and water equivalent. Model 26 has the same snow layers, in the same sequence, but the ice layer is absent. The r-values for all of these models versus frequency in the range 10^7 to 10^8 Hz are shown in figure 40. Although the curves overlap, the effect of the ice layer in modifying the response is quite evident, and particularly for the model with the ice absent.

Model 27. A(0.2)/B(0.2)/C(0.2)/D(0.2)/E(0.2)/F(0.2)/G(0.2)/VI
Model 28. G(0.2)/F(0.2)/E(0.2)/D(0.2)/C(0.2)/B(0.2)/A(0.2)/VI
Model 29. A(0.2)/G(0.2)/B(0.2)/F(0.2)/C(0.2)/E(0.2)/D(0.2)/VI
Model 30. Composite (1.4)/VI

The seven snow types A through G have progressively increasing dielectric constants and conductivities. Models 27 through 29 are composed of layers 0.2 m thick of each snow type, arranged first in the order of increasing dielectric constant, next in the order of decreasing dielectric constant, and finally interspersed. Model 30 represents a composite snow whose electrical thickness is equal to that for the preceding models. The r-values versus frequency in the range of 10^7 to 10^8 Hz are shown in figure 41. As one would expect, the respective curves show a dependence on the snow sequence.

Model 31. A(0.2)/B(0.2)/C(0.2)/D(0.2)/E(0.2)/F(0.2)/G(0.2)/I*
Model 32. G(0.2)/F(0.2)/E(0.2)/D(0.2)/C(0.2)/B(0.2)/A(0.2)/I*
Model 33. A(0.2)/G(0.2)/B(0.2)/F(0.2)/C(0.2)/E(0.2)/D(0.2)/I*
Model 34. Composite (1.4)/I*

For models 31 through 34, the same comments apply as for the models 27 through 30. The r-values versus frequency in the range of 10^7 to 10^8 Hz are shown in figure 42.

Model 35. Dielectric Constant Proportional to Depth (24 layers plus earth)

The effect of gradual increase in dielectric constant with depth is analyzed in model 35. A total depth of snow of 2.4 m is assumed, whose dielectric constant varies uniformly from the value 1.0 at the top ($y = 0$) to the value 5.0 at the bottom ($y = 2.4$). The total depth, for the computer calculations, is taken to be divided into 24 layers, each 0.1 m thick. The dielectric constant for each layer is taken to be the value at the middle; mathematically:

$$K_y = 1.00 + \frac{4}{2.4} y \qquad (24)$$

and $y_1 = 0.05$, $y_2 = 0.15$, $y_3 = 0.25$, etc. The dielectric constants for the 24 successive layers (starting with the top one) are, therefore, 1.08; 1.25; 1.42; 1.58; 1.75; 1.92; 2.08; 2.25; 2.42; 2.58;

2.75; 2.92; 3.08; 3.25; 3.42; 3.58; 3.75; 3.92; 4.08; 4.25; 4.42; 4.58; 4.75; and 4.92. The earth dielectric constant is taken to be 15.0. The snow and the earth are assumed to have values of tan δ about 10^{-5} for the frequency being investigated.

Model 36. Dielectric Constant Proportional to Height (24 layers plus earth)

Model 36 is the same as the preceding, except that the dielectric constant is assumed to be 1.0 at the earth, and to vary uniformly to the value 5.0 at the top of the snow. As before, for the computer calculations 24 layers are assumed, each 0.1-m thick. The dielectric constant for each layer is obtained from the sequence of model 35, starting with the bottom one. The snow and the earth are assumed to have the same tan δ values as for the preceding model. For clarity, we list the successive dielectric constants, starting with the top one and progressing lower: 4.92; 4.75; 4.58; 4.42; etc.

Model 37. Interspersed Layering (24 layers plus earth)

This model employs the same set of dielectric constants as for the preceding two models, but the layers are assumed to be interspersed. Starting with the top layer and proceeding downward, the dielectric constants of the successive layers are: 2.92; 3.08; 2.75; 3.25; 2.58; 3.42; 2.42; 3.58; 2.25; 3.75; 2.08; 3.92; 1.92; 4.08; 1.75; 4.25; 1.58; 4.42; 1.42; 4.58; 1.25; 4.75; 1.08; and 4.92. The dielectric constant of the earth is taken to be 15.0.

The values of r in the frequency range 10^7 to 10^8 Hz are given for models 35 through 37 in figure 43. The curves are quite different from each other, as one would expect, because the assumed variations of dielectric constant with depth represent extreme cases. From these purely illustrative cases one obtains some idea of the type of response when the impedance match between air and earth is quite gradual, in comparison to the response when the transition is abrupt. The total electrical thickness and the total water equivalent are constant for models 35 through 37.

MULTILAYERED MODELS BASED ON SNOW COURSE MEASUREMENTS

The multilayered models for this section are based on *in-situ* measurements of the dielectric constant on an existing snow course. Located in the Sierra Nevada mountains, this course is called "Six-Mile Valley." On 14 March 1973 vertical profiles of snow density and dielectric constant were taken. The dielectric constant was taken with a capacitance meter, that operated at about 5×10^6 Hz; plates of the meter were inserted into the side wall of a hand-dug pit. The measured profiles of density and dielectric constant are given in figure 44. From the latter profile it appears that a layer of wet snow was present between the 1.0 to 1.5 m snow height. Similar layering was noted on other snow courses in the vicinity, so the data appear to be trustworthy. Most of the measured courses displayed less variation in dielectric constant with depth, in comparison to Six-Mile Valley data.

From the density and dielectric constant values, we obtain the snow wetness using equation (19). With this information we construct the layer thicknesses and electrical parameters given in table 7. The column labeled "Snow Type" refers to the dependence of the tan δ value on frequency.

Model 38. Original Layering for Six-Mile Valley Snow Course, Earth Type VI

This model represents the measured values for the Six-Mile Valley snow course, given in table 7; earth type VI is employed. Useful information is obtained by examining the effect of a variety of earth types, which is done below.

Model 39. Reverse Layering for Six-Mile Valley Snow Course, Earth Type VI

This model resembles model 38, but with the layering sequence reversed for all layers except layer number 10; the latter is considered to remain next to the earth because its thickness is 0.35 m, while each of the other snow layers has a thickness of 0.20 m. Interchanges of layers 1 through 9 thus demonstrate the effect of electrical parameter interchanges, without thickness changes of any kind.

Starting at the snow top, the layers for model 39 have the following sequence of dielectric constants: 1.96; 1.90; 1.78; 1.78; 2.31; 2.38; 2.44; 1.66; 1.54; 1.96; and 20.0.

Model 40. Interspersed Layering for Six-Mile Valley Snow Course, Earth Type VI

This model is the same as model 38, except that layers are interchanged: 1 is followed by 9; 2 is followed by 8; 3 is followed by 7; etc. The result is the following sequence of dielectric constants for model 40: 1.54; 1.96; 1.66; 1.90; 2.44; 1.78; 2.38; 1.78; 2.31; 1.96; and 20.0.

Model 41. Original Layering, Earth Type IV
Model 42. Reversed Layering, Earth Type IV
Model 43. Interspersed Layering, Earth Type IV
Model 44. Original Layering, Earth Type VII
Model 45. Reversed Layering, Earth Type VII
Model 46. Interspersed Layering, Earth Type VII

Models 41 through 46 are intended to show the effect of earth characteristics on the r-values versus frequency. The snow layers are the same as for the corresponding models 38 through 40.

The r-values vs frequency for models 38 through 46 are presented as a group, to expedite intercomparison.

For the frequency range of 10^6 to 10^7 Hz, the r-values are very nearly the same, regardless of the layering sequence. Because of this, only the r-values for the three types of earth (IV, VI, and VII) are given in figure 45. At 10^6 Hz, the snow layers have no discernible effect on the earth r-value.

14

For the frequency range of 10^7 to 10^8 Hz, the r-values for models 38 through 40 are given in figure 46; models 41 through 43 in figure 47; and models 44 through 46 in figure 48. To permit further comparison, models 38, 41, and 44 are given in figure 49. The frequency at which the first minimum occurs is substantially the same for models 38 through 46. This is a consequence of the fact that the electrical thickness of the snow is the same for all of these models.

We now consider the frequency 10^8 to 10^9 Hz. The r-values for models 38, 41, and 44 are shown in figure 50; for models 39, 42, and 45 in figure 51; and for models 40, 43, and 46 in figure 52. We note that for a given earth type, the selected layer sequences produce quite different responses; however, for a given layer sequence, the responses have the same curve forms for all three earth types. We also note that at the frequency of 3×10^8 Hz (midway in the decade being considered) the wavelength in the snow is about 60 to 70 cm, which is about equal to twice any layer thickness (40 cm). Because of this, one would expect that each layer would have a considerable effect in modifying the net response, so that the r-value versus frequency would be quite different for the three layering combinations.

For the frequency range 9.0×10^9 to 10.0×10^9 Hz, the r-values for models 38, 41, and 44 are essentially the same, so only one curve is shown in figure 53. It is noted that the curve has regularly spaced minima, and does not show attenuation. Evidently the wet layers 3, 4, and 5 are sufficiently absorbing that they represent a half-space. However, layers 1 and 2 do not have appreciable attenuation, and so these two layers produce the regularly spaced minima. Using the average dielectric constant of 1.6 for layers 1 and 2 and their combined thickness of 0.4 m, one obtains from equation (10) the value 0.30×10^9 Hz as the spacing between successive minima, which is the value also obtained from figure 53.

Model 47. Snow D Component on Top of Six-Mile Valley Layers

This model, the last to be considered in this paper, is selected to give further evidence of the sensitivity of a swept-frequency system to wetness of snow. Snow E, from table 1, has only 2 percent volume wetness. The effect of this wetness can be demonstrated by rearranging layers 3, 4, and 5 of table 7 so that they are on top of the other layers. Thus for model 47 the layers have dielectric constants, starting with the top layer, of: 2.44; 2.38; 2.31; 1.78; 1.78; 1.66; 1.54; 1.90; 1.96; 1.96; 15.0. Each of the layers is 0.2 m thick, except the one next to the earth, which is 0.35 m thick.

The r-values are shown vs frequency for the range 3.0 to 7.0×10^9 Hz in figure 54. Initially, the r-values show no evident regularity, but above the frequency of about 5×10^9 Hz the r-values approach the value 0.220, which is the r-value for a snow half-space having a dielectric constant of 2.44.

Evidently the characteristics of the model below the wet layers are immaterial in the r-values for frequencies greater than 5×10^9 Hz. This type of behavior confirms the statements made previously in connection with models 38, 41, and 44 for the frequency range of 9×10^9 to 10×10^9 Hz.

DISCUSSION

The illustrative models presented in this paper indicate that snow layering affects the reflection magnitudes of EM waves as follows:

1. For the first minimum, the magnitude and frequency are substantially independent of the layer sequence, or the introduction of measurable loss in the snow.

2. Higher-order minima are quite dependent on details of the model.

The calculation of the parameters of an unknown model from the r values vs frequency (i.e., the "inversion problem") is not in the scope of the present paper, which is limited to the presentation of r vs f curves for illustrative models.

A few comments may be appropriate regarding limitations arising from practical matters. In this context, target characteristics such as size and smoothness may be of concern.

For specular reflection, most of the returned wave comes from the first Fresnel zone, whose area is

$$S = \pi H \lambda / 2 \qquad (25)$$

where H is the aircraft altitude and λ is the transmitted wavelength. For a single homogeneous snow layer, the first dip in the r vs f plot occurs at a wavelength that is four times the snow thickness multiplied by the square root of the dielectric constant. For given layered media, one may use an effective dielectric constant given by

$$K_{\text{eff}} = \left(\frac{\sum_i d_i \sqrt{K_i}}{\sum_i d_i} \right)^2 \qquad (26)$$

where d_i and K_i are the layer thicknesses and dielectric constants, respectively.

As an example, if we assume that a helicopter is at an altitude H of 150 m, and that the snow has a depth of 2 m with an effective dielectric constant of 2, the Fresnel zone area is about 2500 m^2. The free-space wavelength for the first minimum in this case is 11.3 m. If we employ the criterion that the roughness should be less than 0.1λ, then underbrush, boulders, etc. should have a characteristic dimension of about 1 m or less. Even in mountainous regions, there appear to be many locations that satisfy these requirements.

In a practical system, the matter of target characteristics must be analyzed more completely than given in this order-of-magnitude evaluation. For example, the slopes inherent in the various objects contributing to the roughness may be more important than the amplitude of the scatterers.

The remote sensing of snowpack characteristics with a surface-located automatic electromagnetic station may provide information regarding depth, density (from the dielectric constant), and wetness of the snow. The target area can, of course, be properly prepared with regard to smoothness

and the earth electrical parameters measured directly when the snow data are being obtained. Such a system would have the important advantage that the snowpack could be monitored as often as desired, without disturbance to the snow itself.

CONCLUSIONS

In addition to the preceding discussion, let us now consider what conclusions and generalizations appear reasonable, based on theory and the results from the model calculations.

The amplitude reflection coefficient r, plotted against frequency f, exhibits approximately sinusoidal variations that are initially quite uniformly spaced. The first minimum occurs at the frequency f_1 given by equation (3), with the effective dielectric constant given by equation (26). The frequency difference between successive minima is approximately $2f_1$. These relations provide the basis for our *first conclusion:* the "electrical thickness" of the snowpack can be obtained within a tolerance of about ±10 percent. For regions where direct measurements of snowpacks are not obtainable, such approximate information would be useful.

The earth characteristics or the presence of layering within the snowpack do not in the usual cases appreciably affect the electrical thickness value. This conclusion can be explained by noting that at the frequency f_1, the wavelength is about four times the electrical thickness, and so any individual layer necessarily is small compared to the wavelength. The minimum occurs because a 180° phase retardation is accumulated by the wave in traversing the snowpack, being reflected at the snow-earth interface, and retraversing the snowpack. In unusual cases, such as a gradational profile of dielectric constant versus depth, the electrical thickness can be obtained from the variation of r-values over a range of frequencies, in addition to the behavior near the first minimum.

The ripening of a snowpack by heat influx from the top can be evaluated by observation of the time dependence of the wetness of the upper portion of the snowpack. A *second conclusion* of this work is that a layer of snow having one percent (or more) volume percent wetness and a thickness of 0.5 m (or more) can be identified by the variation in r-values in the range of 10^9 to 10^{10} Hz. The presence of such a layer on the top of the snowpack, or under a layer of dry snow, can be demonstrated from the r-values.

The electrical thickness has already been discussed. A *third conclusion* from this paper is that the dielectric constant, averaged over the layers, can be obtained within a tolerance of about ±10 percent from the variation of the r-values with frequency; the depths of the dips (maximum minus minimum r-values) are dependent on the snow and earth dielectric constants, and the latter can be obtained by measurements before and after the first appreciable snowfall. Because the contribution of wetness to the dielectric constant can be identified, the remaining (or "dry") snow dielectric constant can be obtained.

A *fourth conclusion* is that from the snowpack electrical thickness and dielectric constant we can obtain the physical depth and density, and thus the water equivalent.

17

A *fifth conclusion* is that the earth electrical parameters can be obtained even with a thick snow layer present, by use of wavelengths that are long compared to the snow thickness. Such information would reveal whether changes have occurred in the earth properties between measurement.

A *sixth conclusion* is that the presence of discrete layers within a snowpack can be identified by the r-value behavior in the frequency range such that the wavelengths are comparable to the layer thickness. The determination of layer parameters by signature analysis may be possible; this involves the estimation of snowpack layering and its parameters, then calculating the response for the assumed model and comparing it with the measurements.

It should be noted that the models for snowpack and earth combinations are much less complicated than in seismic exploration situations, for which inversion procedures have been successfully developed. Unlike many other profile-inversion situations, the snowpack remote measurement program can include ground-truth data, to aid in model definition.

The essential information that is desired for snowpack water resource management is the water equivalent and wetness. Layering information, per se, is of secondary importance. Keeping in mind possible uncertainties in meteorological forecasts, we conclude that the tolerances of about ±10 percent, discussed above, are quite acceptable.

Ames Research Center
  National Aeronautics and Space Administration
    Moffett Field, Calif. 94035, December 9, 1975

REFERENCES

1. Saxton, J. A.: Reflection Coefficient of Snow and Ice at V.H.F. Wireless Engineer, vol. 27, no. 316, Jan. 1950, pp. 17—25.

2. Cumming, W. A.: The Dielectric Properties of Ice and Snow at 3.2 Centimeters. J. Appl. Phys., vol. 23, no. 7, July 1952, pp. 768—73.

3. Jiracek, G. R.: Radio Sounding of Antarctic Ice. University of Wisconsin. Geophysical and Polar Research Center, Dept. of Geology. Research Report Series No. 67-1, 1967, pp. 1—127. (Contribution no. 214)

4. Evans, S.; and Smith, B. M. E.: A Radio Echo Equipment for Depth Sounding in Polar Ice Sheets. J. Sci. Instrum. (Journal of Physics, E), ser. 2, vol. 2, no. 2, Feb. 1969, pp. 131—36.

5. Waite, William P.; and MacDonald, Harold C.: Snowfield Mapping with K-band Radar. Remote Sensing of Environment, vol. 1, no. 2, March 1969, pp. 143—50.

6. Linlor, W. I.: Snowpack Water Content by Remote Sensing. In The Role of Snow and Ice in Hydrology. Proceedings of the Banff Symposia, September 1972. Paris, UNESCO; Geneva, WMO; Budapest, IAHS, 1973, vol. 1, pp. 713—26.

7. Linlor, William I.; and Smith, James L.: Electronic Measurements of Snow Sample Wetness. In Santeford, Henry S., and Smith, James L., comp. Advanced Concepts and Techniques in the Study of Snow and Ice Resources. Washington, D.C., National Academy of Sciences, 1974, pp. 720—28.

8. Linlor, W. I.; Meier, M. F.; Smith, J. L.: Microwave Profiling of Snowpack Free-Water Content. In Santeford, H. S., and Smith, J. L., comp. Advanced Concepts and Techniques in the Study of Snow and Ice Resources. Washington, D.C., National Academy of Sciences, 1974, pp. 729—36.

9. Ward, S. H., Jiracek, G. R.; and Linlor, W. I.: Electromagnetic Reflection from a Plane-Layered Lunar Model. J. Geophys. Res., vol. 73, no. 4, Feb. 15, 1968, pp. 1355—72.

10. Linlor, W. I.; Ward, S. W.; and Jiracek, G. R.: Electromagnetic Measurement of Lunar Subsurface Water. In Linlor, William I., ed. Electromagnetic Exploration of the Moon. Proceedings of the Symposium held at NASA-Ames Research Center, Moffett Field, California, June 11—13, 1968. Baltimore, Mono Book Corp., 1970, pp. 157—69.

11. Stratton, Julius A.: Electromagnetic Theory. New York, McGraw-Hill Book Co., Inc., 1941.

12. Colin, L., ed.: Mathematics of Profile Inversion. Proceedings of a workshop held at Ames Research Center, Moffett Field, Calif. 94035, July 12—16, 1971. NASA TM X-62,150, Aug. 1972.

13. Ambach, W.; and Denoth, A.: Studies of the Dielectric Properties of Snow. Zeitschrift für Gletscherkunde und Glazialgeologie, Bd. 8, Ht. 1—2, 1972, pp. 113—23.

14. Mellor, M.: Properties of Snow. U.S. Army Cold Regions Research and Engineering Laboratory, Hanover, N.H. Cold Regions Science and Engineering, pt. III, sect. A1, Dec. 1964.

15. Evans, S.: Dielectric Properties of Ice and Snow — a Review. Journal of Glaciology, vol. 5, no. 42, Oct. 1965, pp. 773—92.

TABLE 1.– ELECTRICAL PARAMETER VALUES

Label	Density, gm/cm^3	K^a	W, %	10^6	10^7	10^8	10^9	10^{10}	σ, mho/m
						Frequency, Hz			
Snow A	0.25	1.50	0	10^{-2}	3.16×10^{-3}	10^{-3}	3.16×10^{-4}	10^{-4}	$\tan\delta$
				8.35×10^{-7}	2.64×10^{-6}	8.35×10^{-6}	2.64×10^{-5}	8.35×10^{-5}	σ
Snow B	.50	2.00	0	10^{-2}	3.16×10^{-3}	10^{-3}	3.16×10^{-4}	10^{-4}	$\tan\delta$
				1.12×10^{-6}	3.52×10^{-6}	1.12×10^{-5}	3.51×10^{-5}	1.12×10^{-4}	σ
Snow C	.50	2.00	0	10^{-1}	3.16×10^{-2}	10^{-2}	3.16×10^{-3}	10^{-3}	$\tan\delta$
				1.12×10^{-5}	3.52×10^{-5}	1.12×10^{-4}	3.52×10^{-4}	1.12×10^{-3}	σ
Snow D	.50	2.21	1	10^{-1}	3.68×10^{-2}	1.35×10^{-2}	5.00×10^{-3}	3.16×10^{-2}	$\tan\delta$
				1.23×10^{-5}	4.52×10^{-5}	1.66×10^{-4}	6.14×10^{-4}	3.88×10^{-2}	σ
Snow E	.50	2.42	2	10^{-1}	4.60×10^{-2}	2.10×10^{-2}	1.00×10^{-2}	6.31×10^{-2}	$\tan\delta$
				1.35×10^{-5}	6.19×10^{-5}	2.83×10^{-4}	1.35×10^{-3}	8.50×10^{-2}	σ
Snow F	.50	2.85	4	10^{-1}	5.80×10^{-2}	3.40×10^{-2}	2.00×10^{-2}	1.26×10^{-1}	$\tan\delta$
				1.59×10^{-5}	9.19×10^{-5}	5.39×10^{-4}	3.17×10^{-3}	2.00×10^{-1}	σ
Snow G	.50	4.13	10	10^{-1}	7.79×10^{-2}	6.18×10^{-2}	5.00×10^{-2}	3.16×10^{-1}	$\tan\delta$
				2.30×10^{-5}	1.79×10^{-4}	1.42×10^{-3}	1.15×10^{-2}	7.26×10^{-1}	σ
Ice	.92	3.20		2.00×10^{-1}	2.00×10^{-2}	2.00×10^{-3}	4.00×10^{-4}	2.00×10^{-3}	$\tan\delta$
				3.56×10^{-5}	3.56×10^{-5}	3.56×10^{-5}	7.12×10^{-5}	3.56×10^{-3}	σ
Earth I			10	10^{-2}	10^{-2}	10^{-2}	10^{-2}	10^{-2}	$\tan\delta$
				5.57×10^{-6}	5.57×10^{-5}	5.57×10^{-4}	5.57×10^{-3}	5.57×10^{-2}	σ
Earth I*			20	10^{-2}	10^{-2}	10^{-2}	10^{-2}	10^{-2}	$\tan\delta$
				1.11×10^{-5}	1.11×10^{-4}	1.11×10^{-3}	1.11×10^{-2}	1.11×10^{-1}	σ
Earth II			10	10^{-1}	10^{-1}	10^{-1}	10^{-1}	10^{-1}	$\tan\delta$
				5.57×10^{-5}	5.57×10^{-4}	5.57×10^{-3}	5.57×10^{-2}	5.57×10^{-1}	σ
Earth III			10	1.0	1.0	1.0	1.0	1.0	$\tan\delta$
				5.57×10^{-4}	5.57×10^{-3}	5.57×10^{-2}	5.57×10^{-1}	5.57	σ
Earth IV			10	10^{-1}	3.16×10^{-2}	10^{-2}	3.16×10^{-3}	10^{-3}	$\tan\delta$
				5.57×10^{-5}	1.76×10^{-4}	5.57×10^{-4}	1.76×10^{-3}	5.57×10^{-3}	σ
Earth V			10	1.0	3.16×10^{-1}	10^{-1}	3.16×10^{-2}	10^{-2}	$\tan\delta$
				5.57×10^{-4}	1.76×10^{-3}	5.57×10^{-3}	1.76×10^{-2}	5.57×10^{-2}	σ
Earth VI			20	10.0	3.16	1.0	3.16×10^{-1}	10^{-1}	$\tan\delta$
				1.12×10^{-2}	3.54×10^{-2}	1.12×10^{-1}	3.54×10^{-1}	1.12	σ
Earth VII			15	1.0	3.16×10^{-1}	10^{-1}	3.16×10^{-2}	10^{-2}	$\tan\delta$
				8.36×10^{-4}	2.64×10^{-3}	8.36×10^{-3}	2.64×10^{-2}	8.36×10^{-2}	σ

[a] Values for K are independent of frequency.

TABLE 2.— REFLECTION AMPLITUDE VALUES FOR SNOW AND ICE

Frequency, Hz	Snow							Ice
	A	B	C	D	E	F	G	
10^6	0.101	0.172	0.175	0.198	0.220	0.258	0.342	0.291
2×10^6	.101	.172	.173	.197	.219	.258	.342	.285
4×10^6	.101	.172	.172	.197	.218	.257	.342	.283
10^7	.101	.172	.172	.196	.218	.257	.342	.283
2×10^7	.101	.172	.172	.196	.218	.257	.341	.283
4×10^7	.101	.172	.172	.196	.218	.256	.341	.283
10^8	.101	.172	.172	.196	.218	.256	.341	.283
2×10^8	.101	.172	.172	.196	.217	.256	.341	.283
4×10^8	.101	.172	.172	.196	.217	.256	.341	.283
10^9	.101	.172	.172	.196	.217	.256	.341	.283
2×10^9	.101	.172	.172	.196	.217	.256	.342	.283
4×10^9	.101	.172	.172	.196	.218	.257	.345	.283
10^{10}	.101	.172	.172	.196	.218	.260	.359	.283

TABLE 3.— ONE METER OF SNOW ON EARTH IV

Frequency, Hz	No snow	Snow						
		A	B	C	D	E	F	G
1.0×10^6	0.521	0.521	0.521	0.521	0.521	0.521	0.521	0.521
2.0	.520	.520	.519	.520	.520	.520	.520	.520
3.0	.520	.519	.518	.519	.519	.519	.519	.518
4.0	.520	.518	.517	.518	.518	.517	.517	.516
5.0	.520	.518	.516	.517	.516	.516	.515	.514
6.0	.520	.517	.514	.515	.514	.514	.513	.511
7.0	.520	.516	.512	.513	.512	.511	.510	.507
8.0	.520	.515	.510	.511	.510	.508	.506	.503
9.0	.520	.513	.507	.509	.507	.505	.502	.497
10.0	.520	.512	.505	.506	.504	.502	.498	.492

TABLE 4.– ONE METER OF SNOW ON EARTH VI

Frequency, Hz	No snow	Snow						
		A	B	C	D	E	F	G
1.0×10^6	0.901	0.901	0.901	0.901	0.901	0.901	0.901	0.900
2.0	.882	.882	.881	.881	.881	.881	.881	.880
3.0	.869	.868	.867	.867	.867	.867	.866	.864
4.0	.859	.858	.856	.856	.856	.855	.854	.851
5.0	.850	.849	.847	.847	.846	.845	.844	.839
6.0	.843	.841	.838	.838	.837	.836	.834	.827
7.0	.837	.834	.830	.830	.829	.827	.824	.815
8.0	.831	.827	.823	.823	.821	.819	.815	.803
9.0	.826	.821	.816	.815	.813	.811	.806	.790
10.0	.821	.815	.809	.808	.806	.803	.796	.777

TABLE 5.– TWO METERS OF SNOW ON EARTH II OR III

Frequency, Hz	Earth II				Earth III			
	No snow	B	C	G	No snow	B	C	G
1.0×10^6	0.521	0.520	0.521	0.520	0.609	0.606	0.606	0.600
2.0	.521	.518	.519	.516	.609	.601	.602	.587
3.0	.521	.514	.516	.509	.609	.596	.596	.571
4.0	.521	.510	.511	.500	.609	.589	.590	.551
5.0	.521	.504	.506	.488	.609	.582	.582	.527
6.0	.521	.497	.499	.472	.609	.573	.573	.499
7.0	.521	.489	.491	.454	.609	.563	.563	.467
8.0	.521	.480	.482	.434	.609	.552	.552	.430
9.0	.521	.470	.471	.410	.609	.540	.540	.388
10.0	.521	.458	.460	.383	.609	.527	.526	.342

TABLE 6.– SKIN DEPTH IN METERS OF SNOWS A–G

Frequency, Hz	A	B	C	Snow D	E	F	G
1×10^6	7.8×10^3	6.8×10^3	6.8×10^2	6.4×10^2	6.1×10^2	5.7×10^2	4.7×10^2
3×10^6	4.5	3.9	3.9	3.4×10^2	3.0×10^2	2.5×10^2	1.8×10^2
1×10^7	2.5	2.1	2.1	1.8×10^2	1.3×10^2	9.8×10^1	6.0×10^1
3×10^7	1.4	1.2	1.2	9.4×10^1	6.5×10^1	4.2×10^1	2.2×10^1
1×10^8	7.8×10^2	6.8×10^2	6.8×10^1	4.8	2.9	1.7×10^1	7.6×10^0
2	5.5	4.8	4.8	3.2	1.8	9.8×10^0	4.1
3	4.5	3.9	3.9	2.6	1.4	7.1	2.8
4	3.9	3.4	3.4	2.2	1.1	5.7	2.2
5	3.5	3.0	3.0	1.9	9.8×10^0	4.8	1.8
6	3.2	2.8	2.8	1.7	8.7	4.2	1.5
7	2.9	2.6	2.6	1.6	7.8	3.7	1.3
8	2.7	2.4	2.4	1.5	7.1	3.4	1.2
9	2.6	2.2	2.2	1.4	6.6	3.1	1.0
1×10^9	2.5	2.1	2.1	1.3	6.1	2.8	9.4×10^{-1}
2	1.7	1.5	1.5	3.7×10^0	1.8	8.1×10^{-1}	2.7×10^{-1}
3	1.4	1.2	1.2	1.8×10^0	8.5×10^{-1}	3.9	1.3×10^{-1}
4	1.2	1.1	1.1	1.1×10^0	5.1	2.3	7.8×10^{-2}
5	1.1	9.6×10^1	9.6×10^0	7.1×10^{-1}	3.4	1.6	5.2
6	1.0	8.7	8.7	5.1	2.4	1.1	3.8
7	9.3×10^1	8.1	8.1	3.9	1.8	8.5×10^{-2}	2.8
8	8.7	7.6	7.6	3.0	1.5	6.7	2.2
9	8.2	7.1	7.1	2.5	1.2	5.4	1.8
10	7.8	6.8	6.8	2.0	9.7×10^{-2}	4.5	1.5

TABLE 7.– SIX–MILE VALLEY MODEL

Layer number[a]	Thickness,[b] m	K	ρ	W	Snow type
1	0.20	1.54	0.42	0	C
2	.20	1.66	.40	0	C
3	.20	2.44	.48	2	E
4	.20	2.38	.46	2	E
5	.20	2.31	.44	2	E
6	.20	1.78	.46	0	C
7	.20	1.78	.45	0	C
8	.20	1.90	.43	0	C
9	.20	1.96	.50	0	C
10	.35	1.96	.50	0	C
11	Earth	20.0	– –	–	VI

[a]The layers are numbered starting at the top.   [b]The total snow depth is 2.15 m.
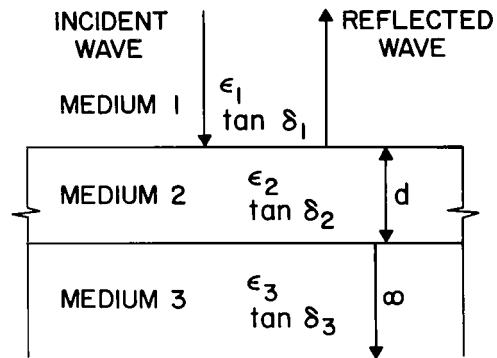
Figure 1.— Three-layered model.
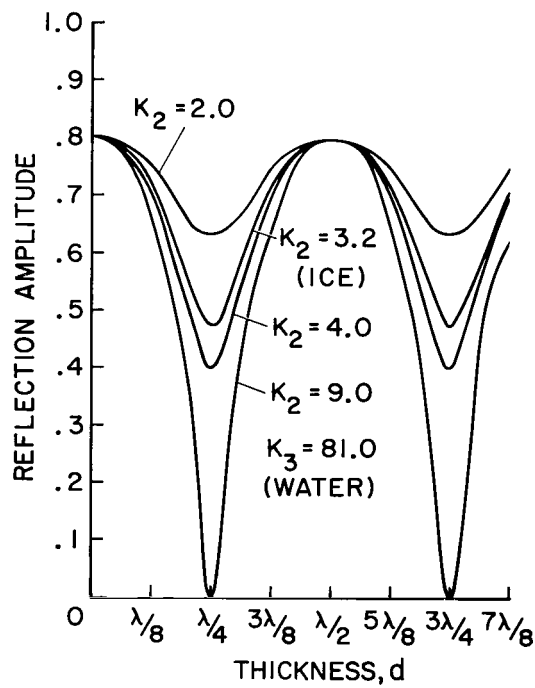
Figure 2.— Reflection amplitude vs thickness.
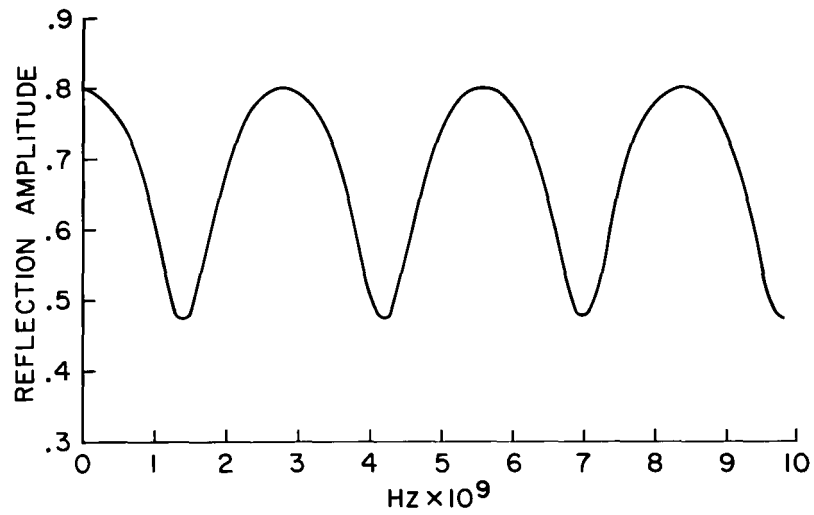
Figure 3.— Ice (0.03 m) over water (pure).
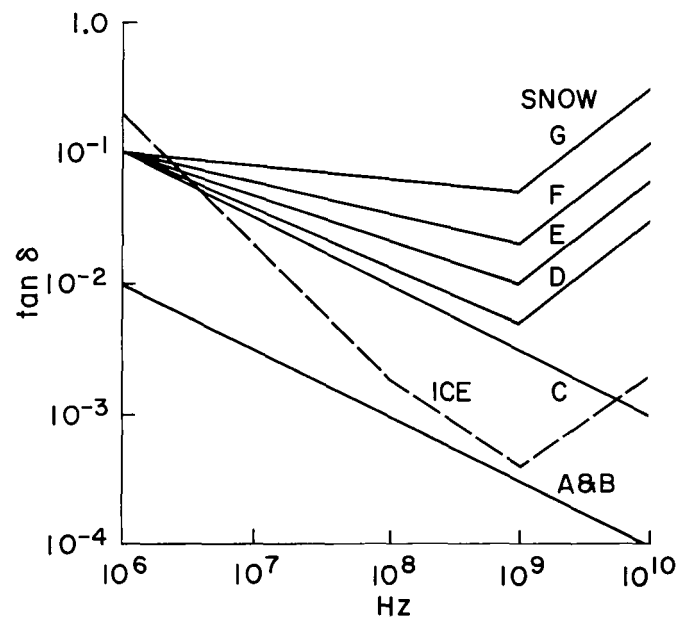
Figure 4.— Snow types and ice.
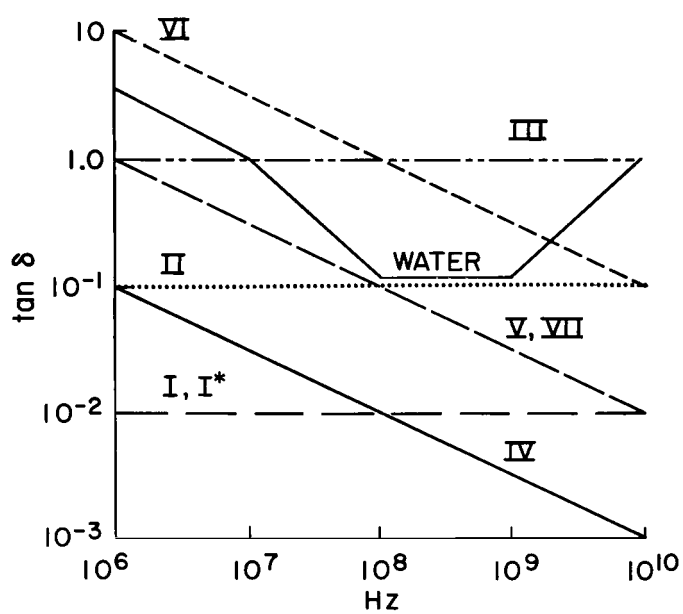
Figure 5.— Earth types and water.
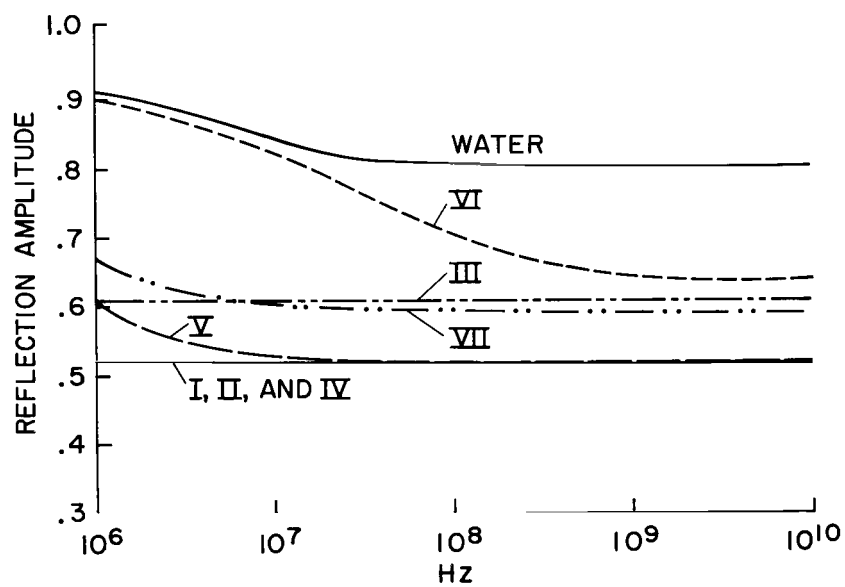
Figure 6.— Earth and water reflection amplitudes.
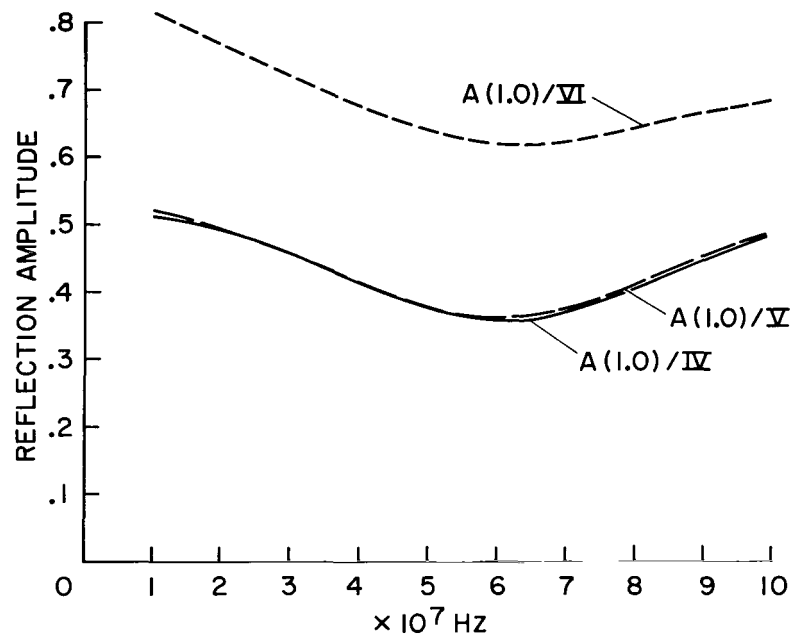
Figure 7.— Snow A (1.0 m) over earth IV, V, and VI.
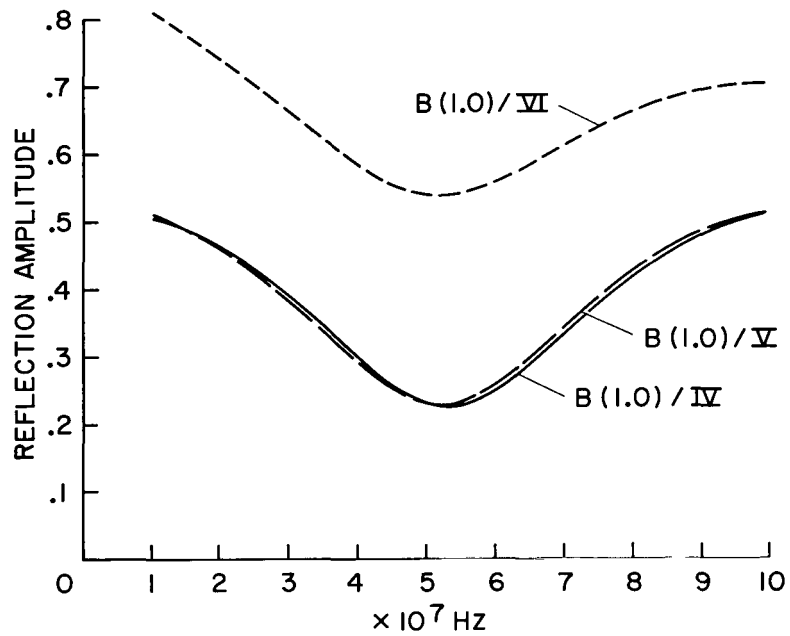
Figure 8.— Snow B (1.0 m) over earth IV, V, and VI.
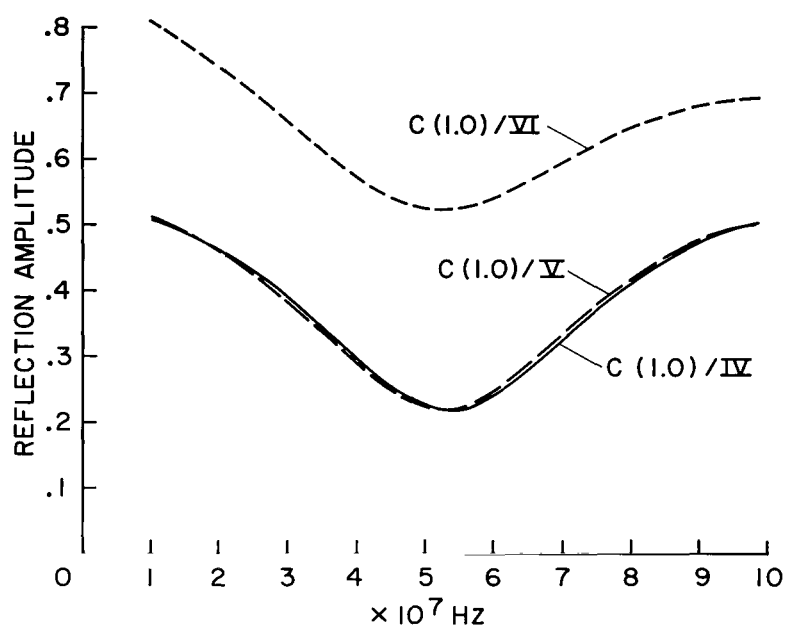
Figure 9.— Snow C (1.0 m) over earth IV, V, and VI.
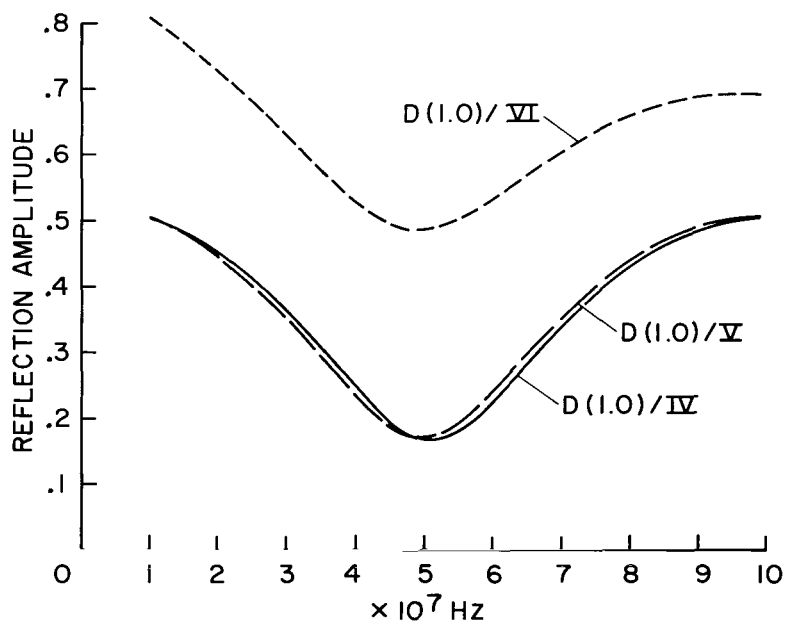
Figure 10.— Snow D (1.0 m) over earth IV, V, and VI.

29
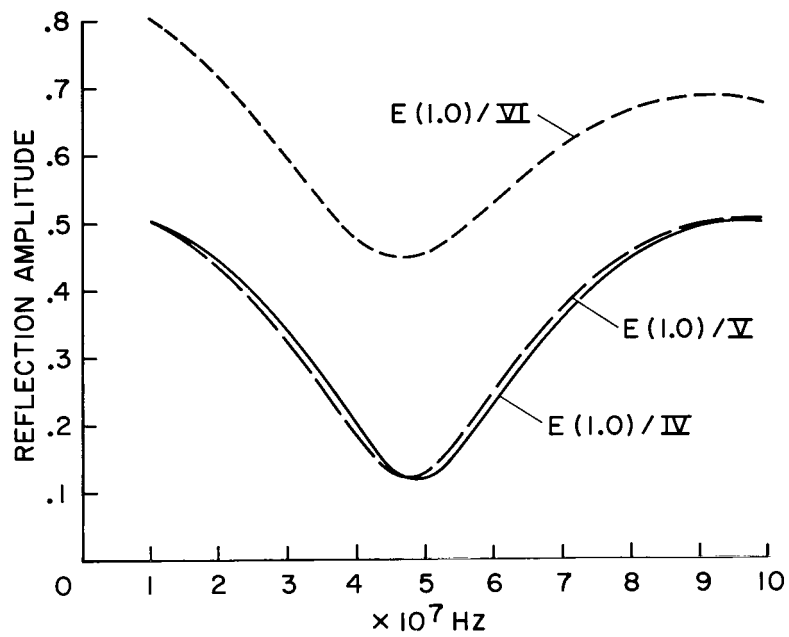
Figure 11.— Snow E (1.0 m) over earth IV, V, and VI.
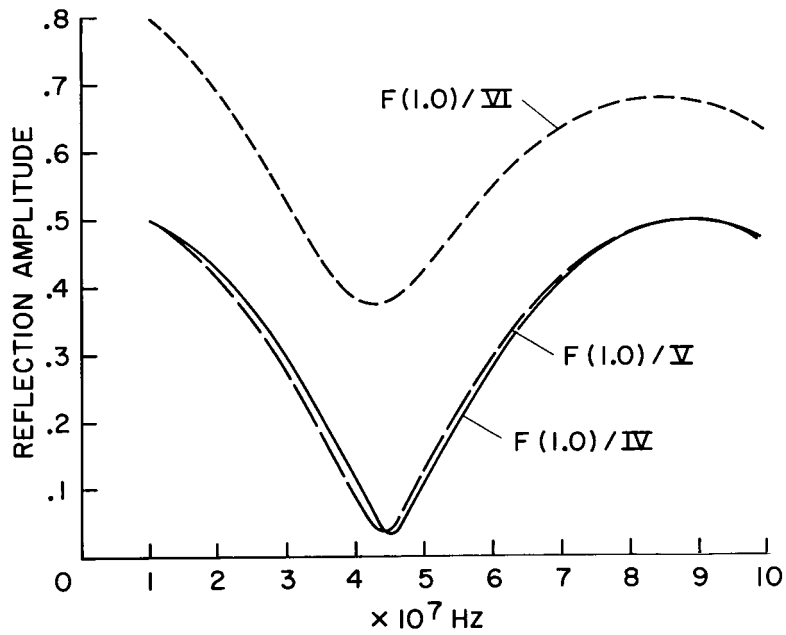
Figure 12.— Snow F (1.0 m) over earth IV, V, and VI.

30
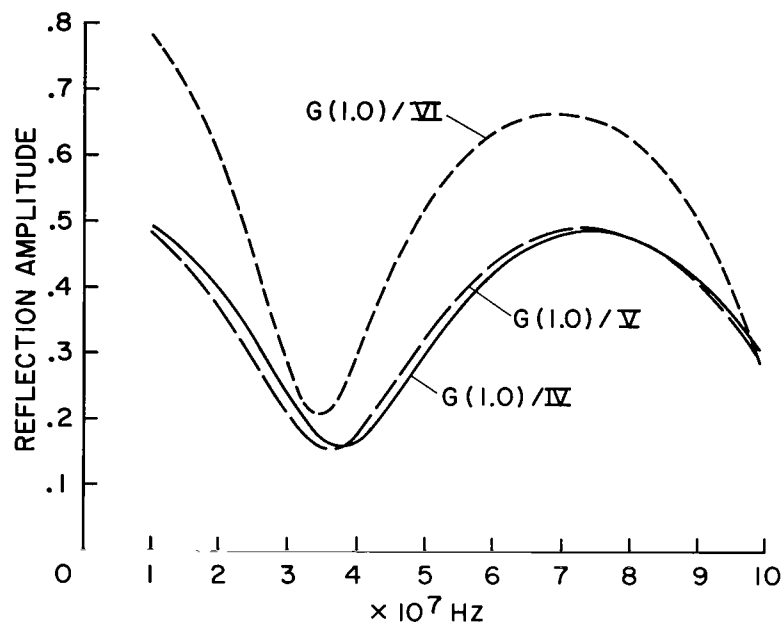
Figure 13.— Snow G (1.0 m) over earth IV, V, and VI.
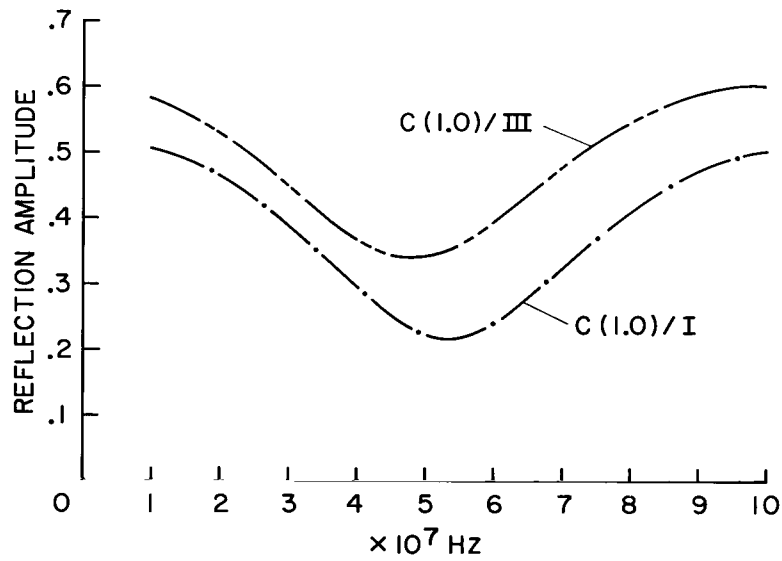
Figure 14.— Snow C (1.0 m) over earth I and III.

31
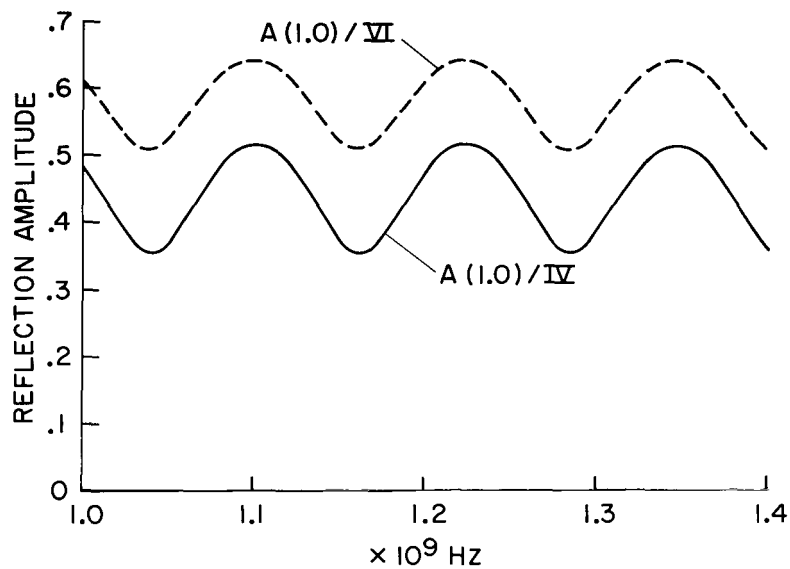
Figure 15.— Snow A (1.0 m) over earth IV and VI.
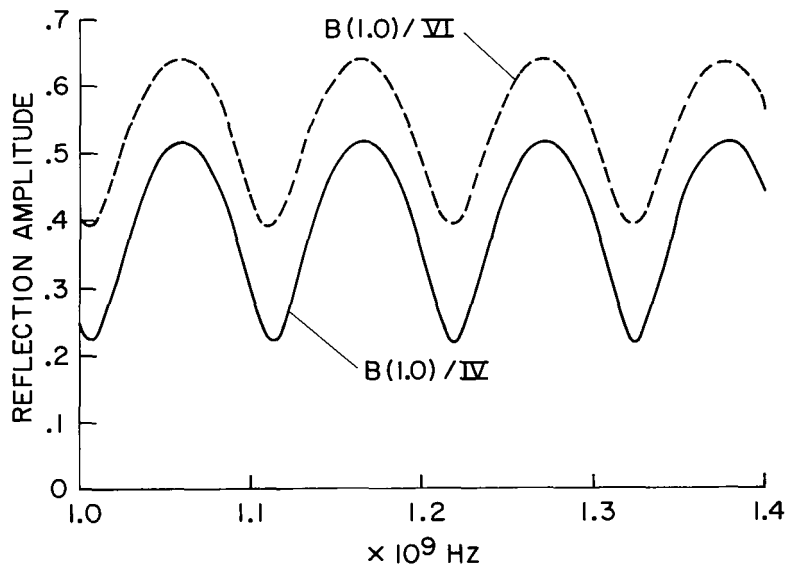
Figure 16.— Snow B (1.0 m) over earth IV and VI.
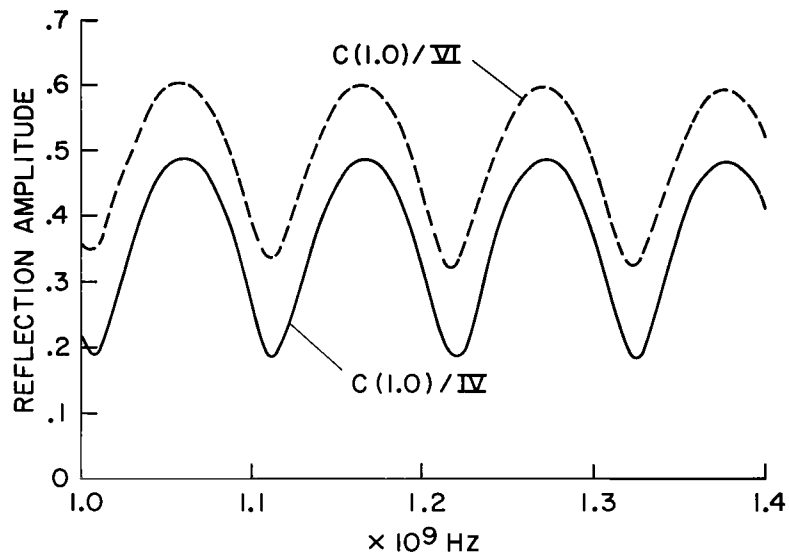
Figure 17.— Snow C (1.0 m) over earth IV and VI.
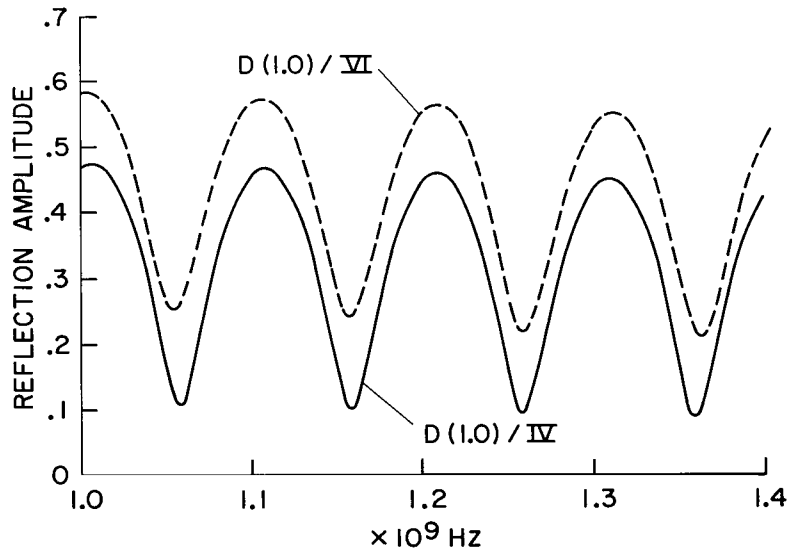
Figure 18.— Snow D (1.0 m) over earth IV and VI.
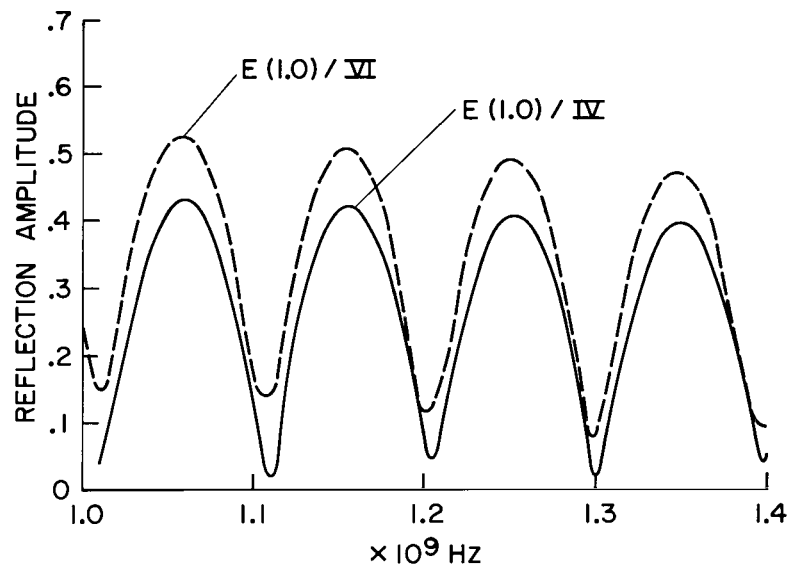
Figure 19.— Snow E (1.0 m) over earth IV and VI.
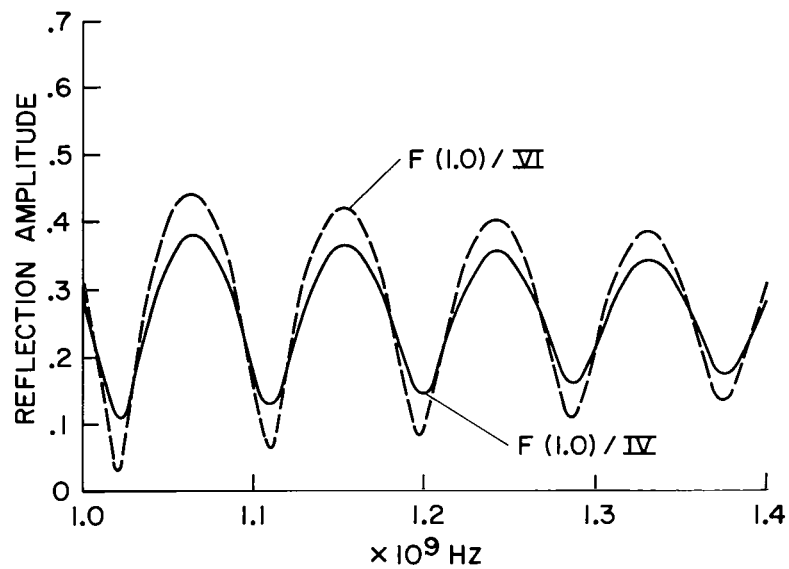
Figure 20.— Snow F (1.0 m) over earth IV and VI.
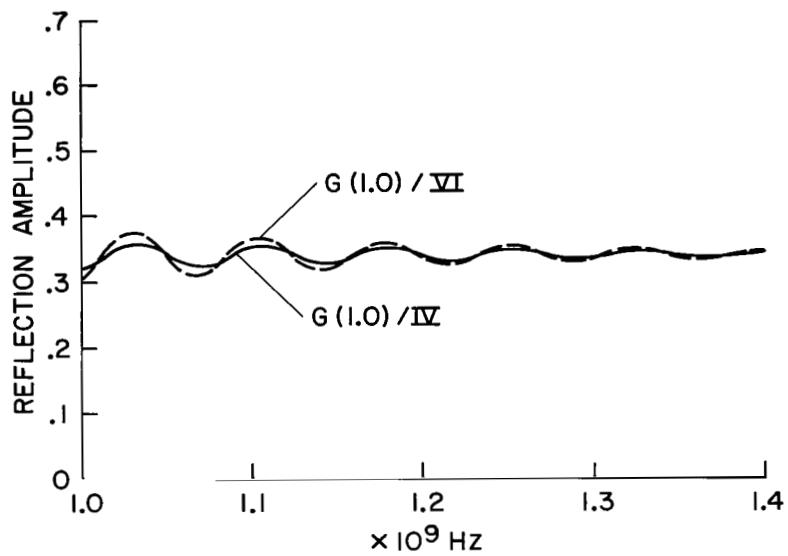
Figure 21.— Snow G (1.0 m) over earth IV and VI.
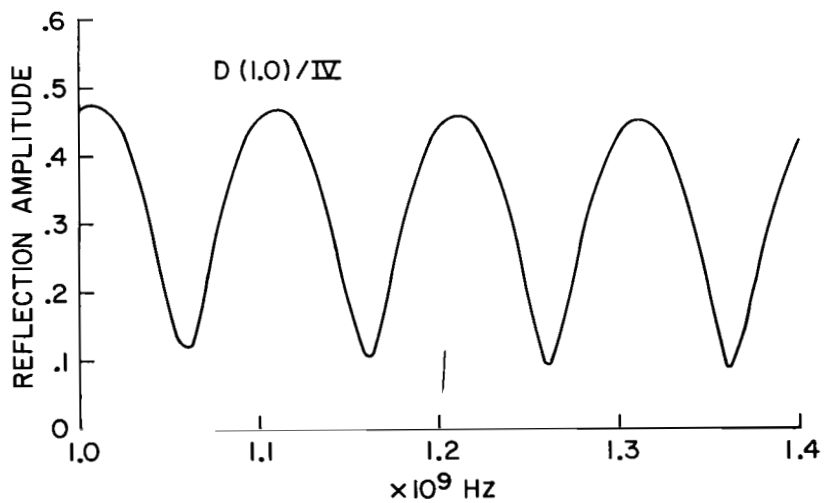
Figure 22.— Snow D (1.0 m) over earth IV.
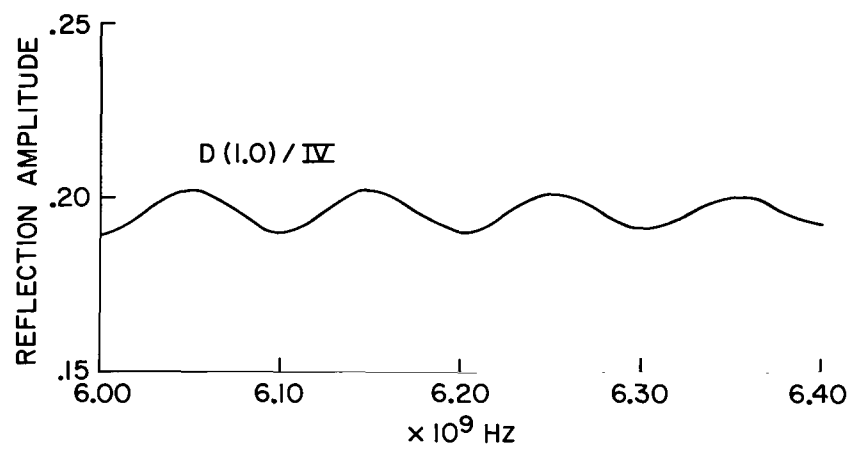
Figure 23.— Snow D (1.0 m) over earth IV.
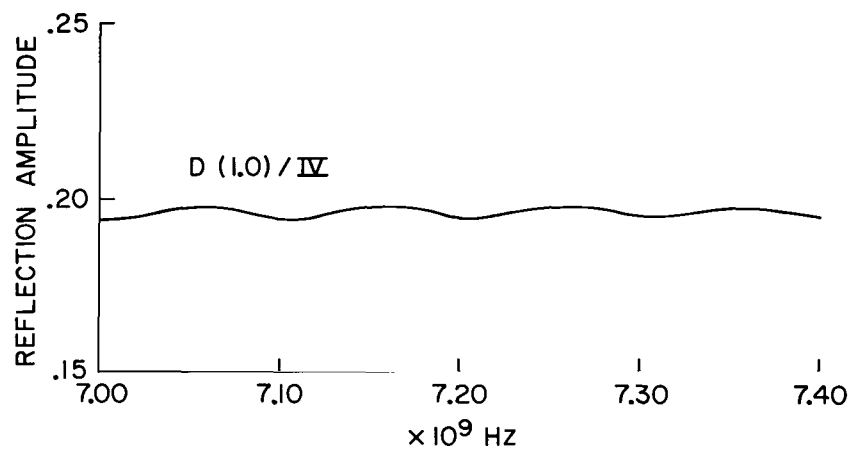
Figure 24.— Snow D (1.0 m) over earth IV.
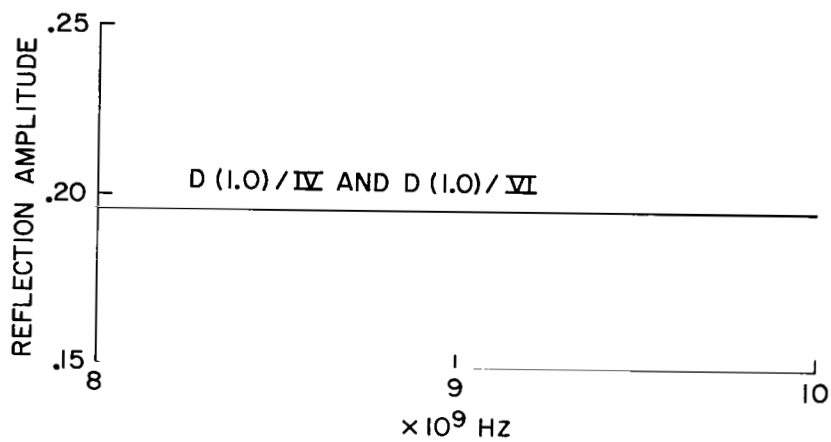
Figure 25.— Snow D (1.0 m) over earth IV and VI.
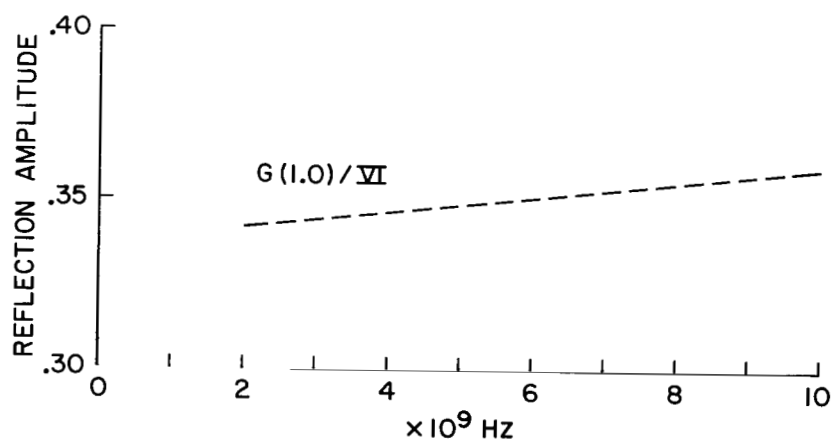
Figure 26.— Snow G (1.0 m) over earth VI.
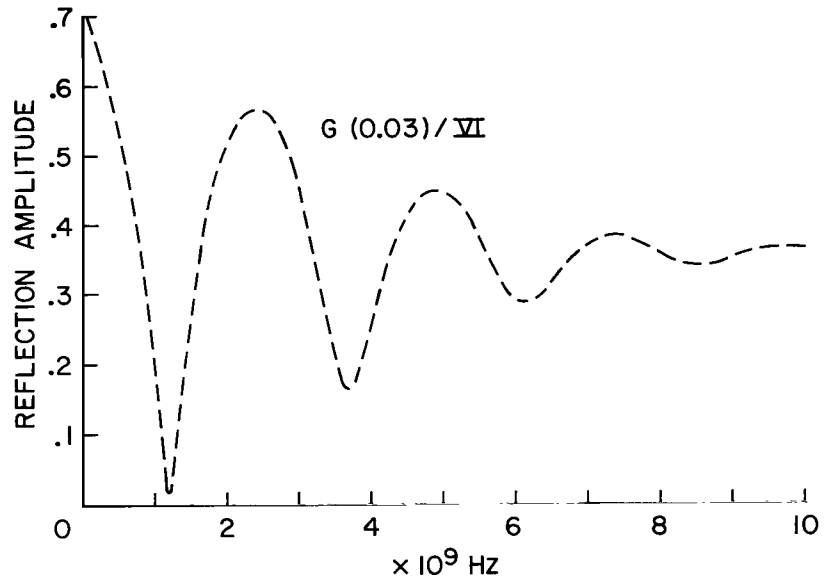
Figure 27.— Snow G (0.03 m) over earth VI.
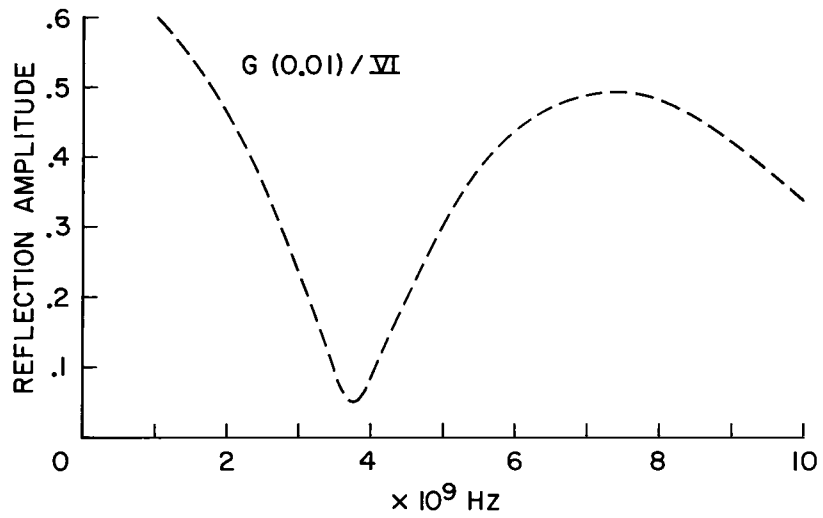
Figure 28.— Snow G (0.01 m) over earth VI.

38
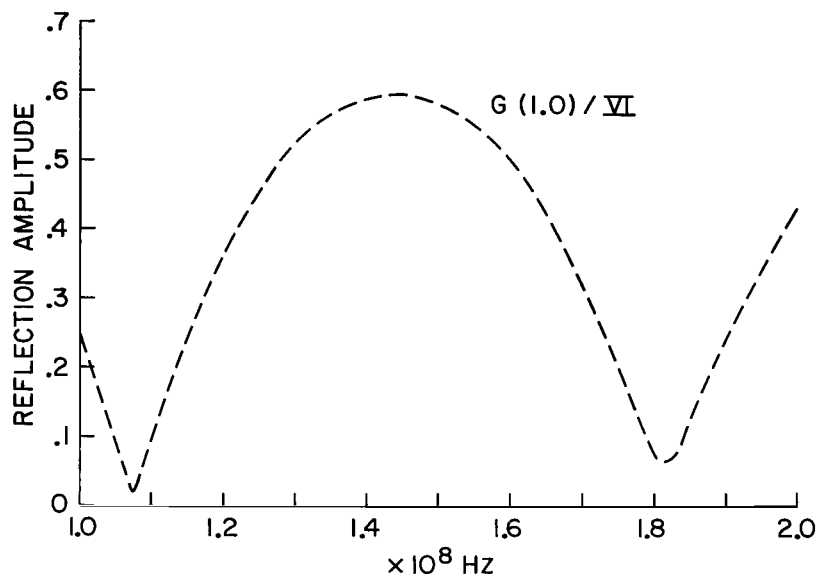
Figure 29.— Snow G (1.0 m) over earth VI.
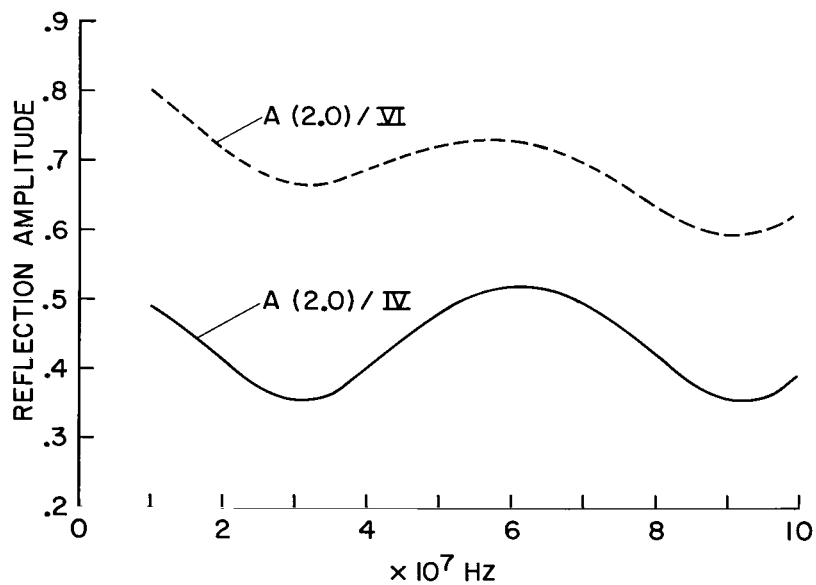
Figure 30.— Snow A (2.0 m) over earth IV and VI.
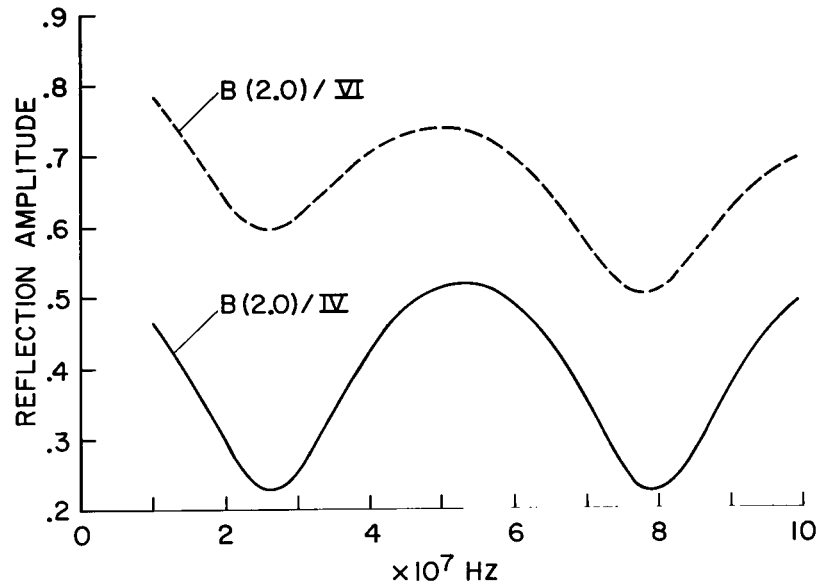
Figure 31.— Snow B (2.0 m) over earth IV and VI.
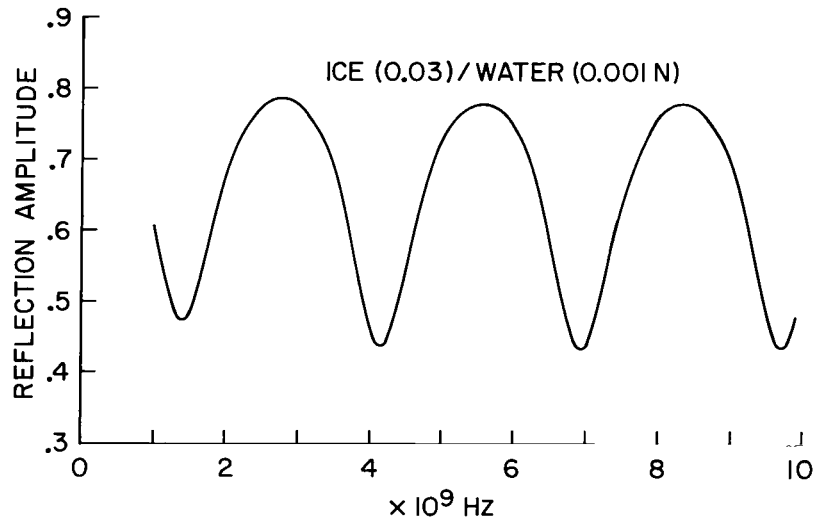
Figure 32.— Ice (0.03 m) over water (0.001 N).
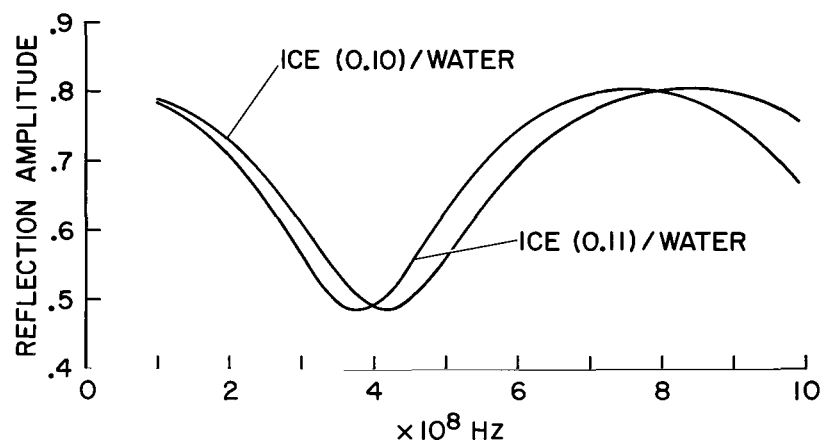
Figure 33.— Ice over water (0.001 N).
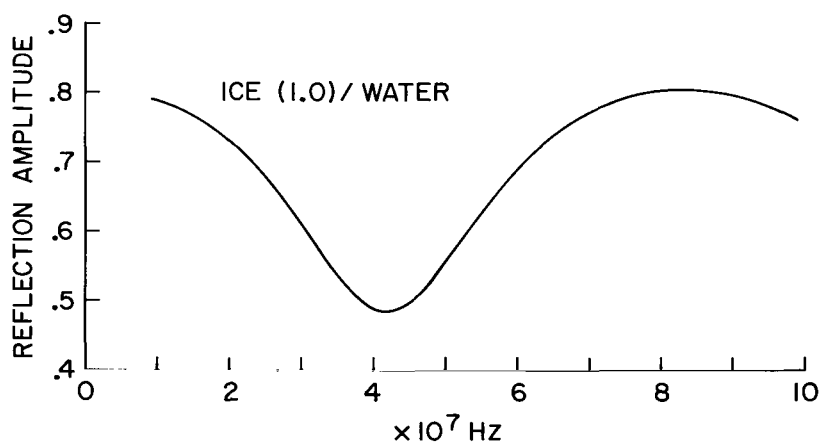
Figure 34.— Ice (1.0 m) over water (0.001 N).
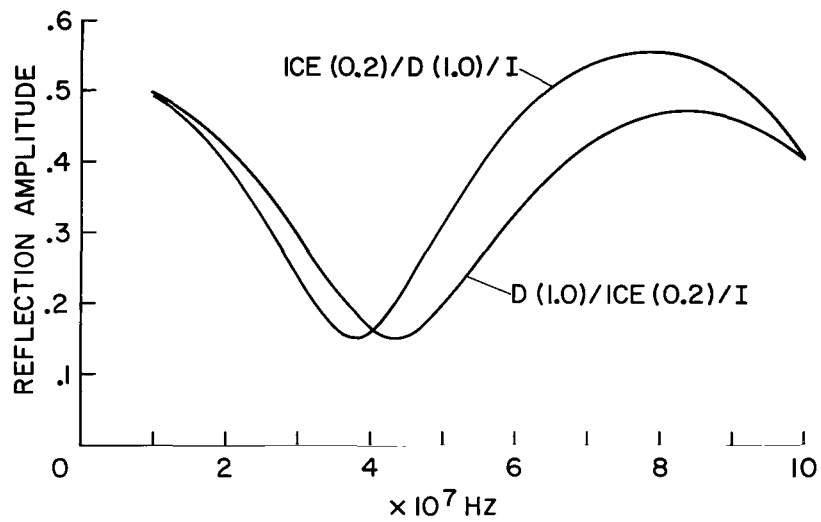
Figure 35.— Snow D (1.0 m) and ice (0.2 m) over earth I.
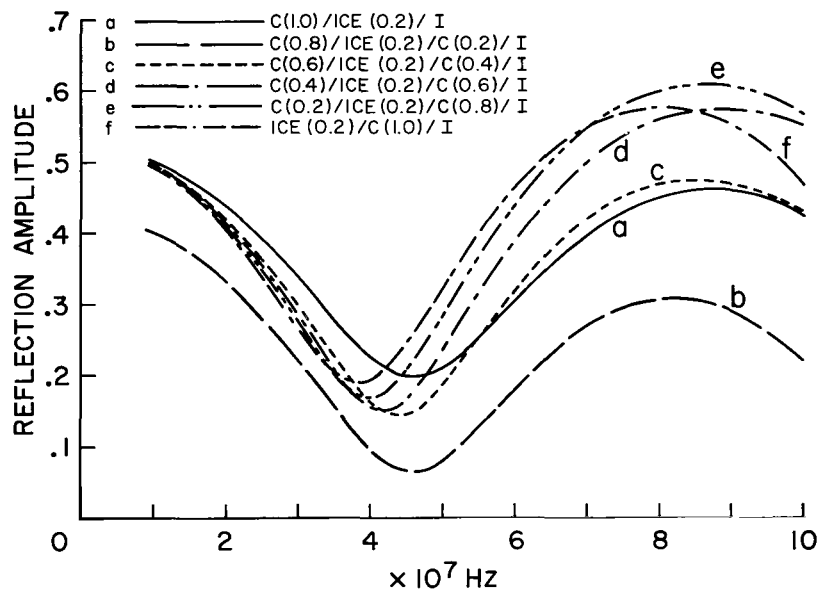
Figure 36.— Snow C (1.0 m) and ice (0.2 m) over earth I.
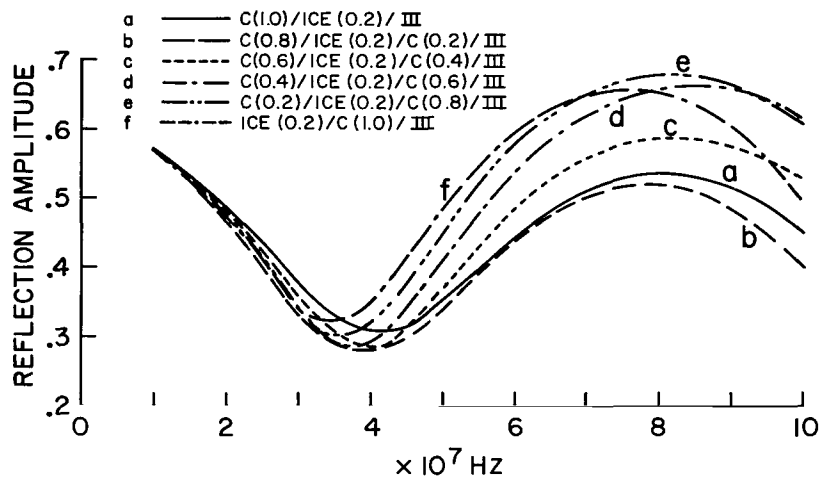
Figure 37.— Snow C (1.0 m) and ice (0.2 m) over earth III.
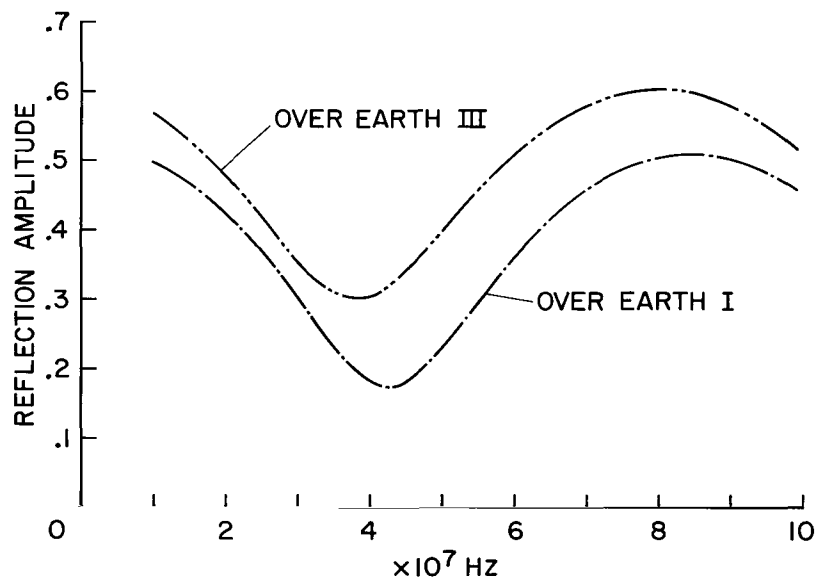
Figure 38.— Composite snow over earth I and III.
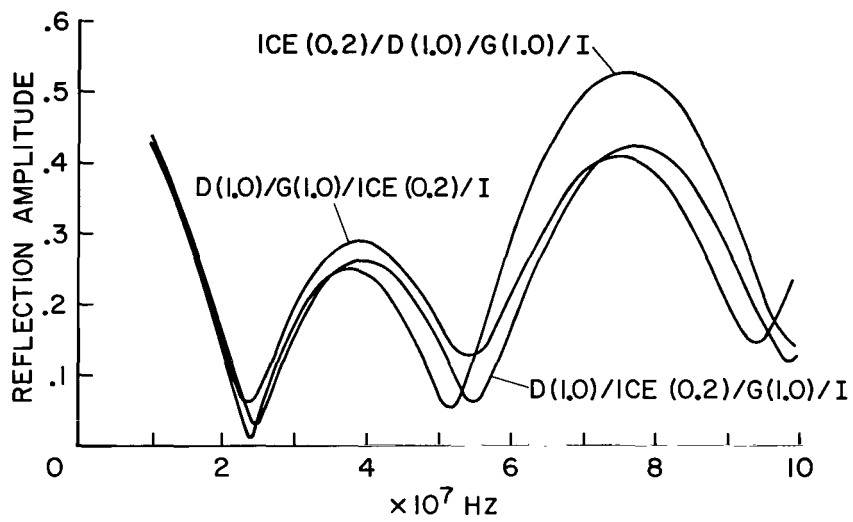
Figure 39.— Snow D (1.0 m), snow G (1.0 m) and ice (0.2 m) over earth I.
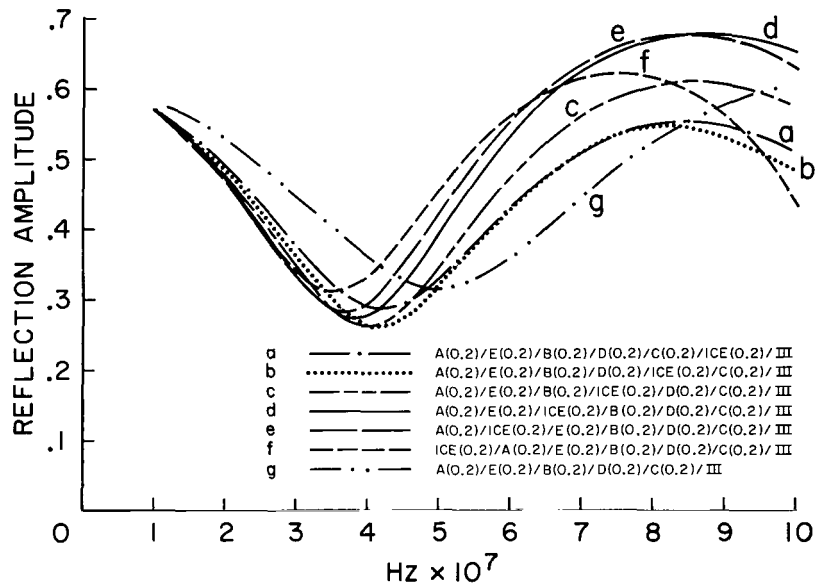
Figure 40.— Snows A, B, C, D, E, and ice over earth III.
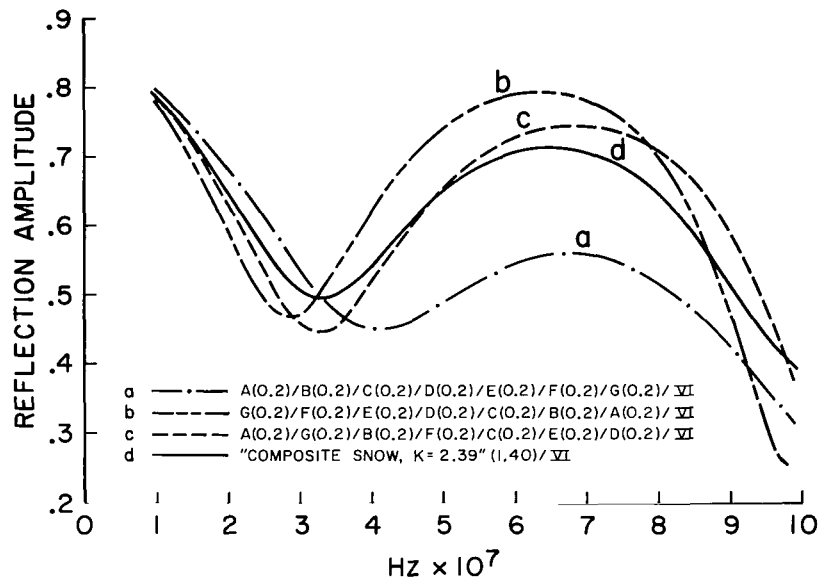
Figure 41.— Snows A, B, C, D, E, F, and G over earth VI.
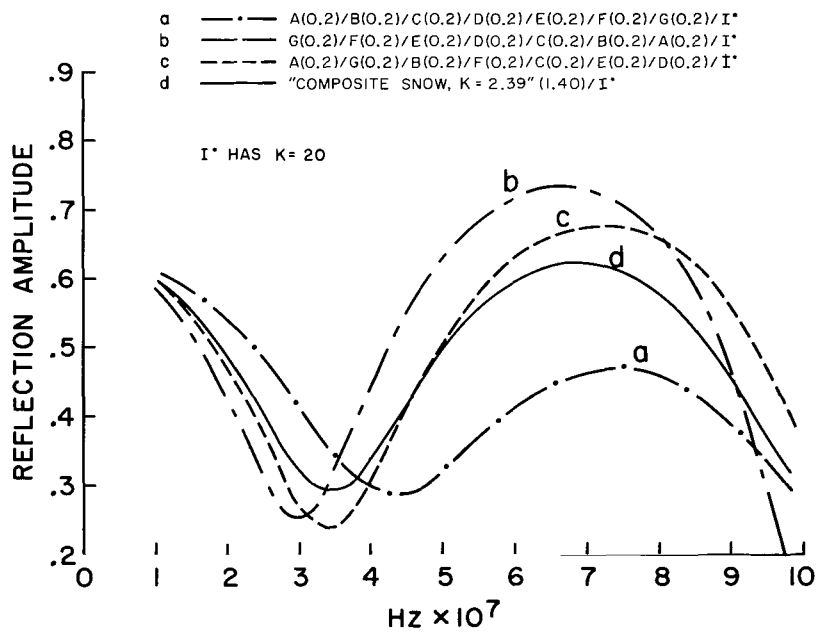
Figure 42.— Snows A, B, C, D, E, F, and G over earth I*.

$$K = 5 - \frac{4}{2.4} y$$

INTERSPERSED

(SEE TEXT)

$$K = 1.00 + \frac{4}{2.4} y$$

REFLECTION AMPLITUDE

HZ ×10^7
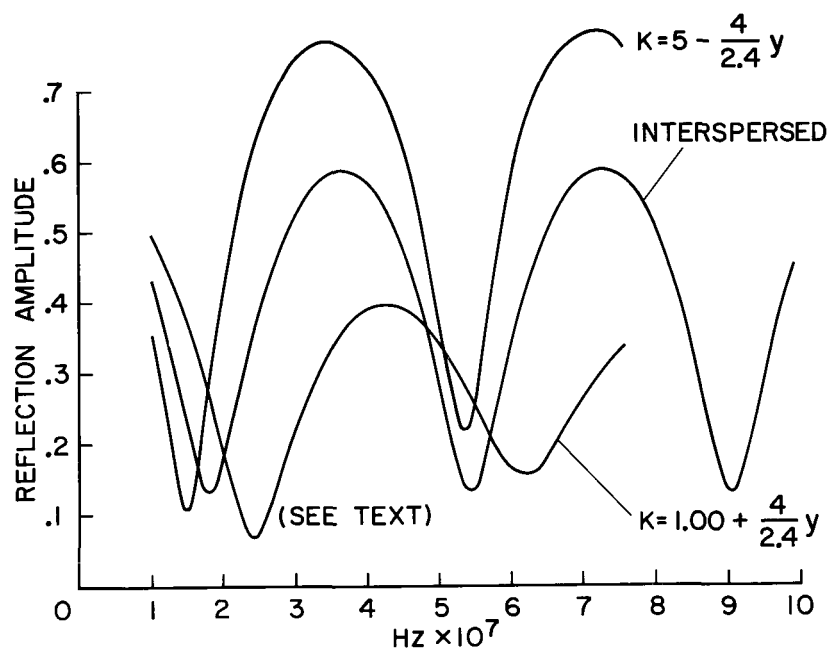
Figure 43.— Snow dielectric constant proportional to depth.

MARCH 14, 1973

TOP OF SNOW

DIELECTRIC
CONSTANT   DENSITY

HEIGHT, cm

DIELECTRIC CONSTANT K →

DENSITY, gm/cm^3 ρ →
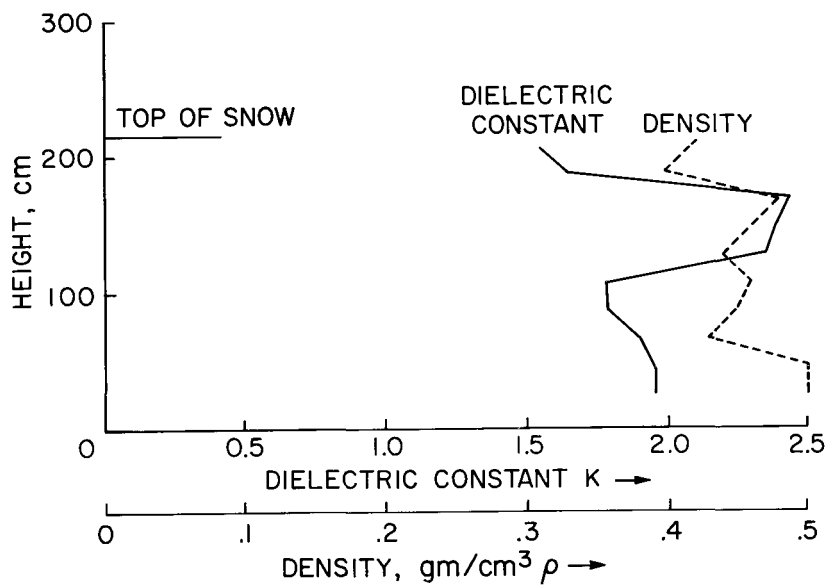
Figure 44.— Six-Mile Valley profiles (ϵ and ρ).
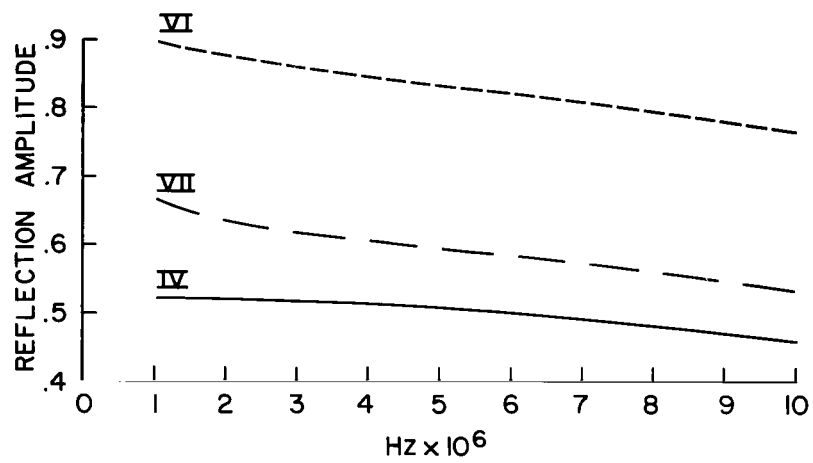
Figure 45.— Six-Mile Valley, original layering on earth IV, VI, and VII.
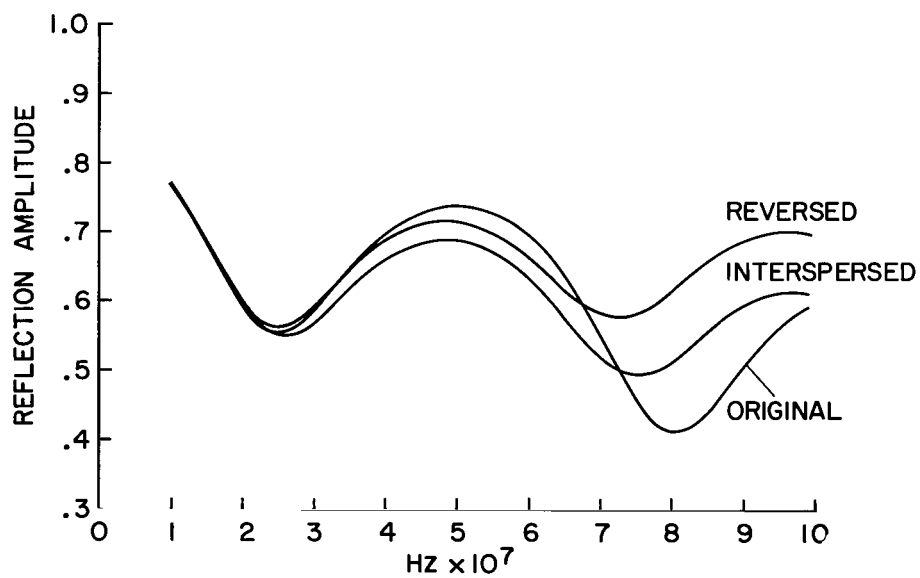
Figure 46.— Six-Mile Valley, layering on earth VI.
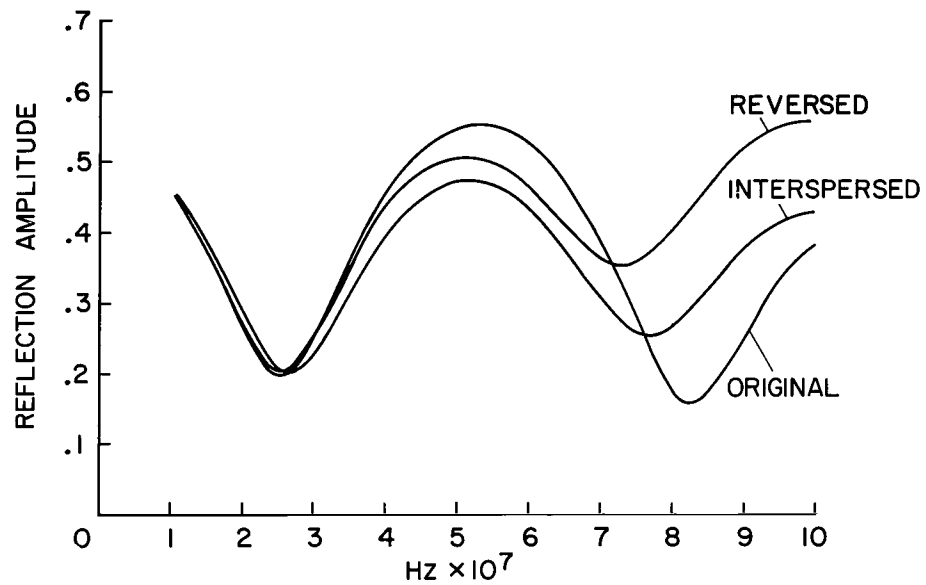
Figure 47.— Six-Mile Valley, layering on earth IV.
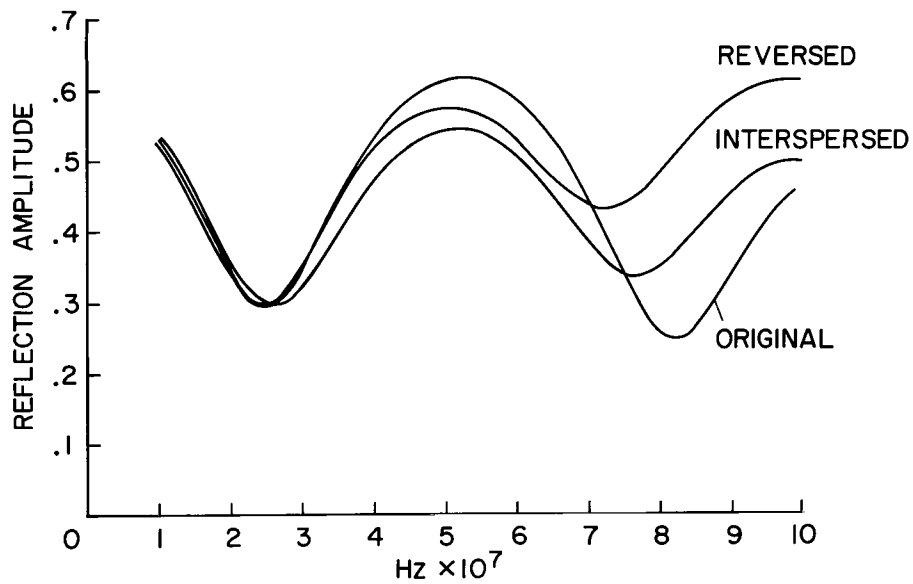
Figure 48.— Six-Mile Valley, layering on earth VII.
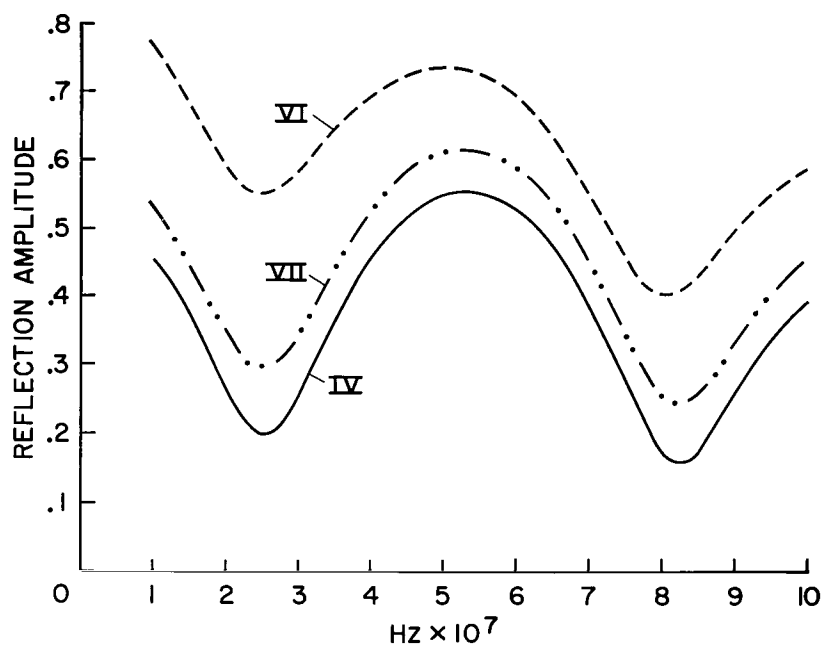
Figure 49.— Six-Mile Valley, original layering on earth IV, VI, and VII.
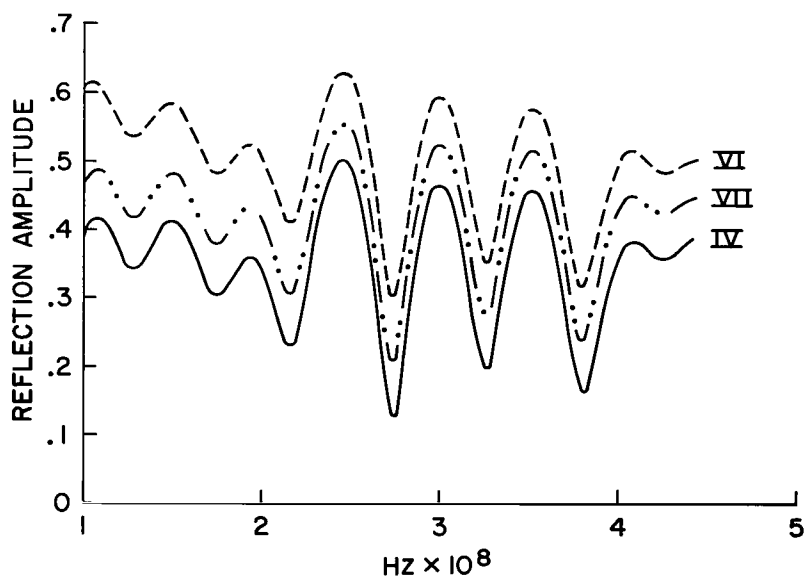
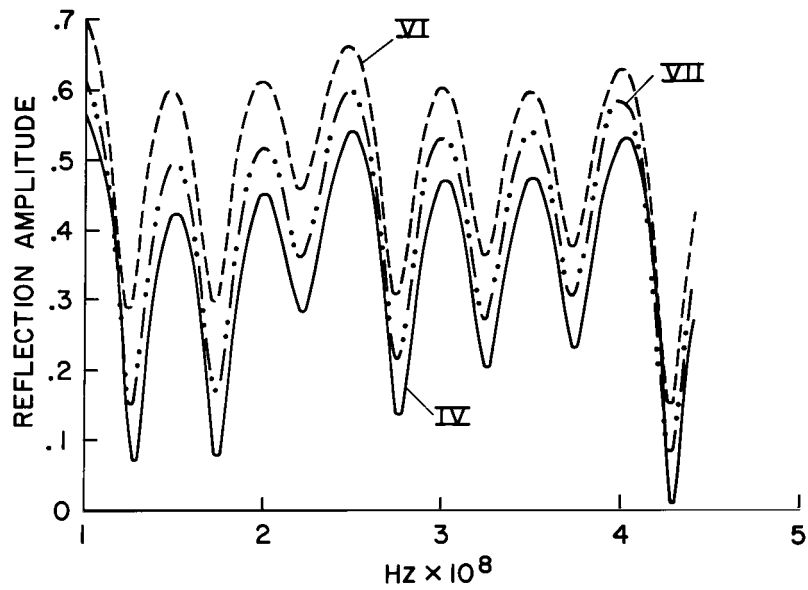Figure 50.— Six-Mile Valley, original layering on earth IV, VI, and VII.

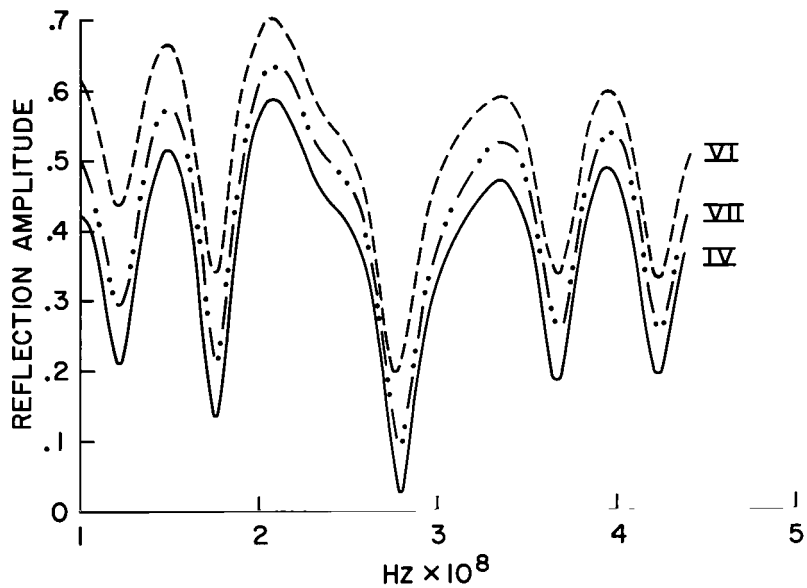Figure 51.— Six-Mile Valley, reversed layering on earth IV, VI, and VII.

Figure 52.— Six-Mile Valley, interspersed layering on earth IV, VI, and VII.
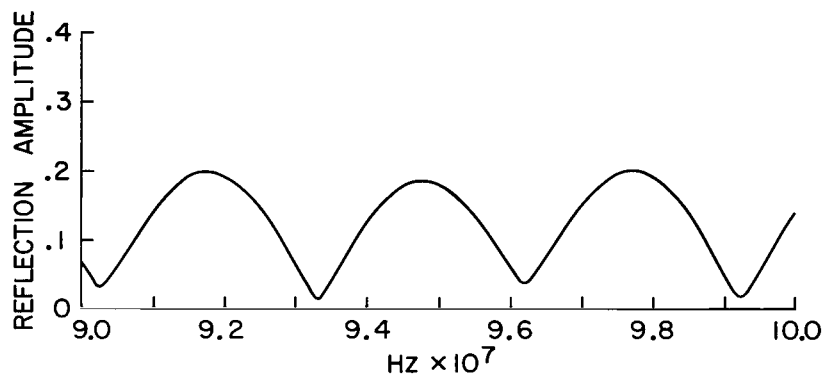
50

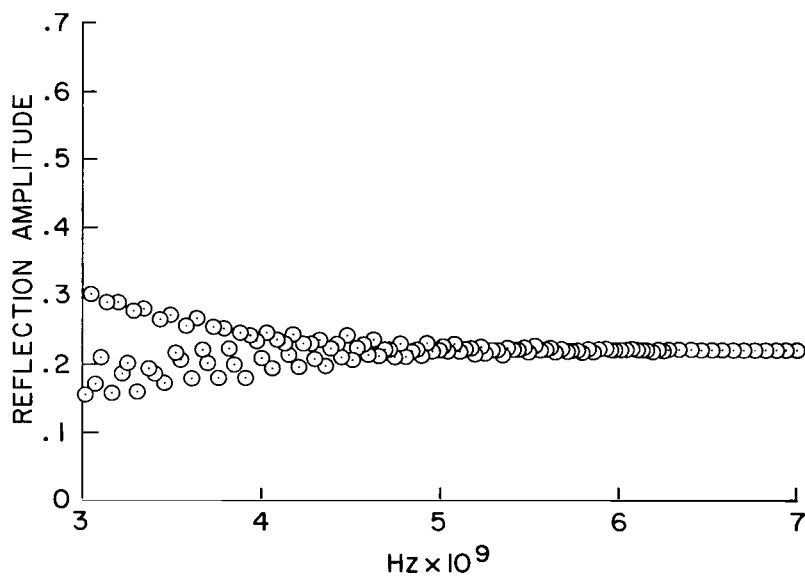Figure 53.— Six-Mile Valley, original layering on earth IV, VI, or VII.

Figure 54.— Six-Mile Valley, snow D on earth IV, VI, or VII.

383 001 C1 U   E 760312 S00903DS
DEPT OF THE AIR FORCE
AF WEAPONS LABORATORY
ATTN: TECHNICAL LIBRARY (SUL)
KIRTLAND AFB NM 87117

*"The aeronautical and space activities of the United States shall be
conducted so as to contribute . . . to the expansion of human knowl-
edge of phenomena in the atmosphere and space. The Administration
shall provide for the widest practicable and appropriate dissemination
of information concerning its activities and the results thereof."*
—NATIONAL AERONAUTICS AND SPACE ACT OF 1958

NASA SCIENTIFIC AND TECHNICAL PUBLICATIONS

TECHNICAL REPORTS: Scientific and
technical information considered important,
complete, and a lasting contribution to existing
knowledge.

TECHNICAL NOTES: Information less broad
in scope but nevertheless of importance as a
contribution to existing knowledge.

TECHNICAL MEMORANDUMS:
Information receiving limited distribution
because of preliminary data, security classifica-
tion, or other reasons. Also includes conference
proceedings with either limited or unlimited
distribution.

CONTRACTOR REPORTS: Scientific and
technical information generated under a NASA
contract or grant and considered an important
contribution to existing knowledge.

TECHNICAL TRANSLATIONS: Information
published in a foreign language considered
to merit NASA distribution in English.

SPECIAL PUBLICATIONS: Information
derived from or of value to NASA activities.
Publications include final reports of major
projects, monographs, data compilations,
handbooks, sourcebooks, and special
bibliographies.

TECHNOLOGY UTILIZATION
PUBLICATIONS: Information on technology
used by NASA that may be of particular
interest in commercial and other non-aerospace
applications. Publications include Tech Briefs,
Technology Utilization Reports and
Technology Surveys.

Details on the availability of these publications may be obtained from:

SCIENTIFIC AND TECHNICAL INFORMATION OFFICE

NATIONAL AERONAUTICS AND SPACE ADMINISTRATION

Washington, D.C. 20546